NACA TN 3412

NATIONAL ADVISORY COMMITTEE FOR AERONAUTICS

TECHNICAL NOTE 3412

CREEP AND CREEP-RUPTURE CHARACTERISTICS OF SOME RIVETED AND SPOT-WELDED LAP JOINTS OF AIRCRAFT MATERIALS

By Leonard Mordfin

National Bureau of Standards

Washington

June 1955

1P

NATIONAL ADVISORY COMMITTEE FOR AERONAUTICS

TECHNICAL NOTE 3412

CREEP AND CREEP-RUPTURE CHARACTERISTICS OF SOME RIVETED AND SPOT-WELDED LAP JOINTS OF AIRCRAFT MATERIALS

By Leonard Mordfin

SUMMARY

Equipment and test techniques which were used in the creep testing of lap joints are described. Riveted aluminum-alloy joints fabricated from 75S-T6 and 24S-T3 sheet with 24S and 24S-T31 rivets were tested at 300°, 400°, and 500° F. Spot-welded joints of 1/4-hard, type 301 stainless steel were tested at 800° F. Each type of joint was also tested in tension at room temperature.

The test results show that the creep of the riveted joints is considerably greater than the creep of the unriveted sheet although not so large that the creep of the sheet is negligible compared with that of the joints. The shapes of the creep curves of the joints indicate that a correlation may be possible with the creep properties of its component materials.

The limited data obtained indicate that the creep-rupture strength of a riveted joint may be approximated by assuming the creep-rupture efficiency of a joint at any temperature to be equal to the room-temperature efficiency. An empirical relation based on the experimental results is proposed to give more accurate estimates of the creep-rupture strength.

The creep at 800° F of spot-welded joints of cold-worked austenitic stainless steel is found to be negligible, at least up to about 200 hours.

INTRODUCTION

The development of jet- and rocket-powered aircraft and the subsequent penetration of the sonic barrier magnified the problem of aerodynamic heating to the point where it is now a major obstacle preventing the attainment of even higher speeds. Many of the materials and components of aircraft construction undergo severe weakening effects at the

elevated temperatures produced by aerodynamic heating. One such effect is creep, the phenomenon of continuing deformation with time under constant loading.

The original method of designing against creep involved the use of stresses so low that creep would be negligible. This, however, violated the minimum weight requirements of aircraft. Accordingly, aircraft structures are now designed with stresses only low enough to prevent excessive deformation or rupture within a specified lifetime. This new criterion obviously requires a more complete knowledge of the creep properties of materials and structures than did the former.

Many experimental investigations have been conducted to determine the creep characteristics of aircraft materials. (See bibliography.) The results of this work are insufficient, however, to describe adequately the deformations and times to rupture of composite structures. It has been considered necessary, as an intermediate step, to evaluate the creep characteristics of simple structural components, such as joints, in order to predict the creep behavior of composite structures.

To date, creep data relating to joints are meager (refs. 1 and 2). The investigation reported herein on the creep of riveted and spot-welded lap joints was undertaken therefore for the following reasons:

(1) To investigate the general nature of the behavior of joints in creep

(2) To obtain design criteria for joints subjected to creep

(3) To assemble equipment and to develop test techniques necessary for conducting a future comprehensive investigation of the creep of joints

This investigation was conducted at the National Bureau of Standards under the sponsorship and with the financial assistance of the National Advisory Committee for Aeronautics. The author is grateful to the members of the Engineering Mechanics Section of the National Bureau of Standards for their valuable suggestions and encouragement throughout this investigation. The assistance of Mr. J. B. Henry of the Allegheny Ludlum Steel Corporation in the procurement of materials and of Mr. W. S. Cockrell of the Ryan Aeronautical Company in the fabrication of specimens is acknowledged. Thanks are also due Mr. R. M. Kinney of the Baldwin-Lima-Hamilton Corporation for his suggestions concerning the test equipment.

SPECIMENS

Design

The general design of the specimens is shown in figure 1. The gage length of the specimen includes four identical lap joints. This combination of joints eliminates the over-all eccentricity which is inherent in a single lap joint and also offers statistical advantages. The average extension per joint as defined in this report is the extension of the gage length divided by four and is less dependent upon minor fabrication and dimensional differences than the extension of a single joint would be. The time to rupture is, conservatively, the time to rupture for the weakest of the four joints. The data obtained with multiple joints are probably more valuable to the designer than data obtained from a single joint and should also yield less scatter than data from a single joint.

The doublers (fig. 1) are about three to four times as thick as the sheet materials. Relatively thick doublers were used so that all of the creep would be effectively restricted to the sheet materials and the rivets, thus simplifying the interpretation and the application of the results. Furthermore, the use of a heavy doubler served to make the test joints approximate actual aircraft construction more closely, that is, the sheet representing a wing skin and doubler simulating a spar cap.

Four groups of specimens were investigated. These were designated as groups A, B, C, and S, where A, B, and C were riveted aluminum-alloy specimens and group S consisted of spot-welded stainless-steel specimens. The nominal dimensions of the four groups of specimens and the materials of which they were fabricated are given in figure 1 and table 1. The direction of rolling of the sheet and strip materials was in the axial direction of the specimens. Rivet holes were made with a No. 30 drill.

It will be noted that the group A specimens were fabricated with 24S (not heat-treated) rivets. These rivets were available at this laboratory, and the group A specimens were intended primarily for checking the operation of the test equipment at the start of the investigation. The results of those tests on group A specimens in which the test equipment functioned satisfactorily are included in this report. These results are valueless as design data since 24S rivets are probably never used in aircraft, but they do offer some assistance in understanding the creep behavior of riveted joints and in corroborating some of the conclusions derived from the tests of the other riveted specimens.

The aluminum-alloy specimens were fabricated at this laboratory and were riveted by a laboratory mechanic having considerable experience in the riveting of various types of aircraft structures. The stainless-steel

specimens were also fabricated at this laboratory, with the exception of the spot-welding, which was done by the Ryan Aeronautical Company.

Each specimen was given a designation such as, for example, 4B-8.7, where the first digit represents the nominal test temperature in hundreds of degrees Fahrenheit, the letter specifies the specimen group in accordance with table 1, and the last figures represent the nominal test load in hundreds of pounds. The example given, then, refers to a specimen of group B, tested at 400° F with a load of 870 pounds. For the specimens statically tested at room temperature, the first digit is replaced by R to indicate room temperature and the last figures are replaced by S to indicate static testing.

Mechanical Properties

Three rivets of each of the two types used in the fabrication of the riveted specimens were tested in shear at room temperature using a conventional hardened-steel double shear jig. The results of these tests are given in table 2.

One specimen of each of the four groups (table 1) was tested in tension at room temperature. The load-extension curves are presented in figures 2(a) and 2(b), the extensions being average values per joint. Table 3 gives the maximum loads obtained in these tests and also the tensile strengths of the unriveted sheets of the specimens computed from data in reference 3. The last column in table 3 lists the room-temperature efficiencies of the joints, which are the ratios of the strengths of the joints to the strengths of their unriveted sheets.

All of the room-temperature tests were performed in a Baldwin-Southwark 20,000-pound-capacity hydraulic testing machine.

CREEP TEST EQUIPMENT

Loading

Two creep testing machines were used. These were converted from two screw-power, beam-and-poise testing machines by the addition of load-maintaining circuits. The two machines are a 50,000-pound-capacity Riehle and a 50,000-pound-capacity Tinius Olsen.

The load-maintaining circuits have been in use at this laboratory for many years and are fully described in reference 4. Briefly, however, the load is maintained as follows: When the test load is applied, the

beam A is balanced at the center of the trig loop B (fig. 3). Thereafter, if the load increases or decreases, the beam moves up or down, respectively, within the trig loop, thereby closing electrical contacts C or D. This causes the loading motor of the testing machine to reduce or apply load, respectively, bringing the load back to the nominal test load and balancing the beam once more. Tests showed that this apparatus maintains load constant within ±5 pounds of the nominal test load.

Serrated wedge grips were used to hold the specimens in the machine. Tests on a dummy specimen at room temperature with SR-4 strain gages showed that the load was applied axially with no bending and that the strain distribution across the width of the specimen was uniform within 5 percent at a distance of 3 specimen widths from each of the grips.

Switches were installed on the machines to cut off the loading motors when rupture of the specimens occurred.

Heating and Temperature Measurement

Two cylindrical electric resistance furnaces, one for each testing machine, were constructed. Nichrome coils were externally wound on Alundum cores. The coils are held in place with refractory cement and surrounded by perlite insulation. Each assembly is enclosed in a cylindrical stainless-steel shell having transite cover plates. The furnaces are mounted upon tables in the testing machines.

The resistance coils are wound in separate sections, each section shunted by an adjustable resistor or a variable autotransformer. These were used to regulate the relative amounts of heat supplied by the different portions of the furnace and thus made it possible to minimize the temperature gradients along the gage lengths of the test specimens. The amount of power supplied to the furnaces was regulated by two potentiometer-type automatic temperature controllers.

Four Chromel-Alumel thermocouples were attached to each specimen with small clamps, one adjacent to each of the four joints. (The thermocouple locations are indicated in fig. 1.) One of these thermocouples was used as the sensing element for the automatic temperature controller, and its output was recorded automatically. The other three thermocouple outputs were measured with a millivolt potentiometer.

Extension Measurement

Two creep extensometers (see fig. 4) were mounted on each specimen, one on each face. The extension occurring in the gage length is transferred by extension arms A and B to the outside of the furnace. These

extension arms are mounted on the specimen with knife edges C and are held in place by tying with Nichrome wire D. This wire has sufficient elasticity at elevated temperatures to hold the extension arms in place even after the thickness of the specimens diminished because of loading. The relative motion of the two extension arms is measured with the scale and vernier combination E. Rollers inserted between the inner and the outer extension arms and between the inner extension arms and the specimen permit the necessary relative motion of the arms. This motion requires a force of about 2 pounds, which is negligible compared with the total loads applied to the specimens.

The extensometers can be read to 0.001 inch with a probable accuracy of ±0.001 inch. This is equivalent to an average extension of 0.00025 inch per joint or an average strain of 0.00022 inch per inch.

Time to Rupture

Switches were attached to the testing machines in such a way that rupture of a specimen opens the circuit of an electric clock. In this manner, the exact time of rupture was obtained even when an observer was not present.

CREEP TEST PROCEDURE

Preparation

Gage lines were lightly scribed on the specimen at the ends of the gage length (fig. 1). The vernier extensometers were mounted. The thermocouples were then clamped to the specimen. The specimen was inserted through the furnace and into the grips. A load of 25 pounds was applied. This was necessary to straighten the specimen so that "zero" extension readings could be made.

Heating and Loading

The specimen was heated to the test temperature while the straightening load was permitted to drop off because of thermal expansion. The aluminum-alloy specimens were heated to test temperature in about 1 hour and the stainless-steel specimens were heated to temperature in about $1\frac{3}{4}$ hours.

After the nominal test temperature was reached, the straightening load was again applied, and the specimen was maintained within 10° F of

constant temperature for 1 hour before the nominal test load was applied. During this 1-hour exposure the temperatures in the furnace had an opportunity to become stabilized, and final adjustments of the furnace controls were made to minimize the temperature gradients along the gage length of the specimen.

At the end of the 1-hour exposure the nominal test load was applied at a crosshead speed of 0.02 inch per second. This was considered time zero for the test. The test load was thereafter held constant with the load-maintaining apparatus, which applied or reduced load, as necessary, at a crosshead speed of 0.2 inch per hour.

Measurements

The first extension measurements were made at room temperature after the 25-pound straightening load was applied. Measurements were again made immediately after the specimen reached the nominal test temperature and the 25-pound load was again applied. These two sets of measurements were used to compute the thermal expansion of the joints, as will subsequently be described. Another set of measurements was made at the end of the 1-hour exposure period to determine whether any creep had occurred during the exposure due to the straightening load. None was detected. Measurements were again made immediately after the nominal test load was applied to determine the initial or "instantaneous" extension.

Extension was measured periodically thereafter until failure. No provision was made for obtaining the extension at rupture, and, from the nature of the specimens, extension measurements after rupture are impossible.

Temperature measurements with the four thermocouples were made at time zero, at half-hour intervals during the first 2 hours, and thereafter every time extension measurements were made.

REDUCTION OF DATA

Temperature Data

Each time temperature measurements with the four thermocouples were made, the four temperatures thus obtained were averaged. This average was called the average specimen temperature for that particular time. The maximum difference obtained between the average specimen temperature and the temperature at any of the four thermocouple locations at that time was 5° F, which was obtained with specimen 3B-12.5 for a period of

$1\frac{1}{2}$ hours. For the duration of most of the tests, however, this difference was less than 3° F.

The average specimen temperatures for each of the tests were maintained constant within 8° F in the worst case, specimen 4C-6.8, and within 3° F in most cases. These temperature variations were not cyclic, for the most part, but were caused by occasional rapid changes of room temperature. As such, they were eliminated in short times by the automatic temperature controllers and did not appear to influence the creep curves.

The mean of the average specimen temperatures for each test was termed the average test temperature.

Extension Data

The extension occurring within the gage length of each specimen was measured with each of the two vernier extensometers mounted upon it. The creep extensions obtained with the two extensometers agreed within 5 percent. The average of these two values, divided by four, was taken as the average extension per joint. This quantity was used in the analyses of the results and in all the tables and figures in this report.

The difference between the extension measurements made at room temperature and upon attainment of test temperature represents the indicated thermal expansion of the joint. This quantity is the difference between the actual thermal expansion of the joint and the thermal expansion of an equal length of extensometer rod, plus the elastic deformation in the joint due to the temperature change of the elastic and shear moduli. This elastic deformation was computed to be negligible and, hence, the actual thermal expansions of the joints are given by

$$D_a = D_i + C_e L(T_e - T_o) \tag{1}$$

where

D_a actual thermal expansion of joint, in.

D_i indicated thermal expansion of joint, in.

C_e coefficient of linear thermal expansion of extensometer rod, in./in./$^{\circ}$F

L length of joint, $1\frac{1}{8}$ in.

T_e temperature of extensometer rod, $^{\circ}F$

T_o room temperature, $^{\circ}F$

The values of C_e for the various test temperatures were estimated from reference 5. In the computations T_e was taken as the average test temperature. Check tests showed that this introduced an error of less than 3 percent, which was considered negligible.

ELEVATED-TEMPERATURE TESTS AND DISCUSSION OF RESULTS

Twenty-six creep and creep-rupture tests were performed. The loads and the average test temperatures at which each of the specimens was tested are listed in table 4. The loads were selected with the object of producing rupture in the range of times from 1 to 100 hours, although this object was not always attained.

Thermal Expansion

The actual thermal expansions of the joints tested are listed in table 4. The average values for each group of specimens at each temperature are plotted in figure 5. Also given in this figure are theoretical thermal expansion curves which were computed from the standard relation

$$D_t = C_s L\left(T_t - T_o\right) \tag{2}$$

where

D_t theoretical thermal expansion of a joint, in.

C_s average coefficient of linear thermal expansion of the materials of the joint, in./in./$^{\circ}F$

T_t nominal test temperature, $^{\circ}F$

The values of C_s were estimated from data in references 5, 6, and 7. The discrepancies between the actual and the theoretical thermal expansions

in figure 5 are within the accuracy of the estimations of C_e and C_s for equations (1) and (2). This indicates that thermal expansion under uniform temperature does not produce any severe relocation of clearances in a riveted joint and that the thermal expansion can therefore be directly computed.

The magnitudes of the thermal expansions, it should be noted, are far from being negligible insofar as structural analysis is concerned.

Creep of Riveted Joints

In figures 6 to 9 are given the creep curves of the joints tested. These figures do not include the thermal expansions of the joints. A logarithmic time scale was used in the plotting of these curves in order that all the curves of a single group at one temperature could be shown on a single set of coordinates. While this method facilitates the comparison of curves for different loads, it does not show the true shape of the creep curve for the riveted joints. A representative creep curve on Cartesian coordinates is therefore shown in figure 10. It will be noted that the creep curve of a joint thus shown is similar in shape to the creep curve of a plain material in that it has primary, secondary, and tertiary creep stages and in that it does not suffer instantaneous deformations due to slip. Thus, it may eventually be possible to find a correlation between the creep of a riveted joint and the tensile, bearing, and shear creep of its component materials. Such a correlation would be extremely valuable since it would enable the designer to predict the creep of a riveted joint of any design from the results of materials tests alone. At present, bearing and shear creep data on aircraft structural materials do not exist in sufficient quantity to establish or refute such a correlation, but information of this type is presently being obtained at other laboratories (refs. 8 to 10, for example).

Efforts to correlate the creep of the riveted joints with only the tensile creep of its component materials were unsuccessful, presumably because the effects of temperature on the tensile, bearing, and shear properties of a material are not the same (ref. 11). Figure 11 shows a comparison of the creep curves of joints 4B-8.7 and 4C-8.7 with the creep curve of 24S-T3 sheet under approximately the same net tensile stress. The latter curve was taken from reference 12, with the creep strains multiplied by $1\frac{1}{8}$ inches, the length of a joint, to make the extensions more comparable. It can be seen that the creep of the joints is much larger than the creep of the sheet, although not so large that the creep of the sheet is negligible compared with that of the joints.

Creep Rupture of Riveted Joints

The times to rupture (table 4) are plotted on logarithmic coordinates as a function of load in figure 12. Straight lines faired through the plotted points corresponding to each group of joints at each temperature appear to give a reasonably close approximation to the experimental results, particularly insofar as load is concerned. For design purposes, then, the load necessary to produce rupture in a given time can be predicted fairly accurately by a relation of the form

$$P = bt^n \tag{3}$$

where

P load, lb

t time to rupture, hr

and b and n are constants which depend upon the design of the riveted joint and the temperature. A relation of this form should not be used, however, to predict the time to rupture of a joint under a given load, since figure 12 indicates that large errors could result. (The experimental results can be approximated equally well by straight lines on semi-logarithmic coordinates, but this yields an empirical relation which is somewhat more cumbersome than eq. (3).)

The values of b and n, equation (3), which satisfy the curves in figure 12 are listed in table 5. In figure 13 the values of b are plotted against absolute temperature on logarithmic coordinates. This figure shows a linear logarithmic relationship between b and absolute temperature. Expressed mathematically,

$$b = cT^m \tag{4}$$

where T is absolute temperature in $^{\circ}R$ and c and m are constants which depend solely on the design of the joint. Since the designs of the joints are, after all, arbitrary ones, it follows that equation (4) is probably not unique.

Substituting equation (4) into equation (3) yields

$$P = cT^m t^n \tag{5}$$

This relation gives the load necessary to produce creep rupture of an aluminum-alloy riveted joint at any given temperature in any given time.

It should be stated, once more, that large errors would be obtained if equation (5) were used to predict the time to rupture for a given load.

The values of c and m which satisfy the curves in figure 13 are listed in table 5. With the values of c, m, and n listed, equation (5) describes the creep-rupture behavior of the riveted joints tested quite closely. Additional tests would be necessary to investigate the influence of the various design parameters of a riveted joint on c, m, and n. Even more important, however, is the necessity of additional tests to examine the validity of equation (5) for joints of other designs and to determine the temperature and time ranges over which it is applicable.

Initial Extension

The initial extensions of the joints tested are listed in table 4 and shown graphically as a function of load in figures 14 to 16. Since linear extrapolations of these curves would not pass through the origin, it is clear that the applied loads produced extensions beyond the elastic range of the joints. In actual practice, however, joints would not generally be subjected to loads above their yield strengths. Hence, the times to rupture would be greater than those obtained in this investigation. From the times to rupture listed in table 4, it may therefore be tentatively concluded that, if an aluminum-alloy riveted joint of reasonable design is subjected to a load not exceeding its yield strength, the time to rupture will be at least about 60 hours and in some cases more than several hundred hours. This, of course, refers to the yield strength at the temperature in question.

Creep-Rupture Efficiency of Riveted Joints

In figures 17 and 18 the load-rupture curves of figure 12 are replotted together with tensile load-rupture curves for unriveted sheet of the same alloys as those used in the joints. The latter curves were converted from the stress-rupture data in references 12, 13, and 14 by multiplying the stresses by the gross cross-sectional area of the sheets.

The creep-rupture efficiency of a riveted joint is defined as the ratio of the load that produces creep rupture of the joint to the load that produces creep rupture of the unriveted sheet at the same temperature and in the same time. The creep-rupture efficiency was computed for all of the joints represented in figures 17 and 18 except those for which rupture data on unriveted sheet are lacking. For joints 3A-7.1, 3B-15, and 5B-7.7, which failed upon loading, the creep-rupture efficiency was computed using data in reference 11 on the elevated-temperature tensile strength of unriveted sheet after a 1-hour temperature exposure.

The creep-rupture efficiencies are listed in table 6. Also listed are the deviations of the creep-rupture efficiencies from the room-temperature efficiencies. With one exception, joint 3A-6, these deviations are seen to be less than 30 percent. Apparently, in the absence of other information, a rough estimate of the load necessary to produce rupture of a joint at a given temperature in a specific time can be obtained by assuming the creep-rupture efficiency of the joint to be equal to the room-temperature efficiency. The accuracy of this method of predicting the rupture strength of a joint is far less than that given by equation (5), but it has the advantage that no creep-rupture tests of joints are needed, since it is based on tensile stress-rupture data of unriveted sheet much of which is already available. Also, this method holds for short-time strength, whereas equation (5) breaks down when t is zero.

In evaluating the creep-rupture characteristics of a new joint design, both methods could be used advantageously. The approximate method based on the estimated creep-rupture efficiency could be used to select the loads for creep-rupture tests to determine the constants for equation (5).

Creep of Spot-Welded Joints

Table 4 shows an ultimate strength of 4,200 pounds for the spot-welded stainless-steel lap joints at approximately 800° F. The creep curves of these joints at 800° F, figure 9, show that under loads up to 97 percent of the ultimate the creep is negligible, at least for times up to about 200 hours. Data in reference 7 show that in this temperature and time range the creep of austenitic stainless steels is universally small. Apparently, then, the residual stresses and the changes in microstructure produced by the spot-welding do not significantly change the creep properties of austenitic stainless steels.

The specimens tested were fabricated from 1/4-hard material. Since the creep resistance of the 18-8 type steels at temperatures up to 800° F is increased by cold-working (ref. 15), the conclusions reached herein are undoubtedly also true for the 1/2-, 3/4-, and full-hard materials.

Under the original plan of this investigation, it was intended to test group S specimens at 600° and 700° F. However, these tests were dispensed with after the 800° F tests since creep would obviously not have been obtained at the lower temperatures.

Description of Ruptures

The distribution of the ruptures obtained in this investigation among the four joints per specimen appeared entirely random.

All of the group A joints ruptured because of shearing of rivets (specimen (b), fig. 19). The skew position of the upper doubler in this figure was caused by unequal shear creep deformations of the rivets in the upper joint.

With the exception of specimen 5B-7.7, all of the group B joints ruptured by tearing and shearing the sheet as shown by specimen (a), figure 19. Bearing deformations were evident in all of the joints in this group. The skew position of the center portion of specimen (a), figure 19, was caused by uneven deformations in the other joints. Specimen (d), 5B-7.7, ruptured because of shearing of both the sheet and one rivet. Bearing deformations were also evident in the unruptured joints of this specimen.

The group C specimens which were tested at elevated temperature failed by shearing the rivets (specimen (b)). The group C specimen tested at room temperature failed because of shearing of the sheet (specimen (c)). All of the group C specimens suffered bearing creep deformations also. The change in the mode of failure of the group C specimens in going from room to elevated temperature indicates that the shear strength of the 24S-T31 rivets decreases more rapidly with temperature than the shear strength of the alclad 24S-T3 sheet.

The group S joints ruptured by shearing and tearing the sheet (specimen (e)) both at room temperature and at 800° F.

The scratches near the gage lines on some of the specimens in figure 19 were caused by the knife edges of the extensometers at rupture.

Effect of Edge Distance

Edge distance e (fig. 1) is often considered in the design of a riveted joint only in the manner in which it affects the ultimate bearing strength of the sheet. A comparison of the modes of failure and the strengths of the group B and the group C specimens, however, shows that it also has a direct effect upon the force required to produce shear failure in the sheet. Hence, while an edge distance of 2.0 diameters may be expected to develop full bearing strength (ref. 3), it does not necessarily develop full joint strength.

Figure 12 shows that the load-rupture curves of the group B and group C joints at 400° F are not parallel. While the degree of nonparallelism is within the probable scatter of the experimental results, it is

quite possible that the rupture strength of the group C joints does actually decrease more rapidly with time than does that of the group B joints. This would mean, more specifically, that the rupture strength of the 24S-T31 rivets in shear decreases more rapidly than the rupture strength in shear of the 24S-T3 sheet at 400° F. Hence, in time, the difference in strength of the two types of joints would become smaller and thereby minimize the effect of edge distance. It is improbable, however, that the two curves could ever cross.

Recommendations

Several methods of estimating the creep and creep-rupture behavior of joints have been discussed in this report. It should be emphasized, however, that the criteria used for these estimations are based on a very limited number of tests. Thus, while they represent much of the information available at this time on the creep of joints, they should by no means be considered final and should therefore be used with caution. It is recommended that additional investigations of this nature be performed on other designs of joints before final criteria are established. These investigations could, among other things, test the validity of equation (5) and determine whether the creep of joints can be predicted from the creep of its component materials.

The strength of the spot-welded steel specimen at room temperature (table 3) is almost three times greater than the maximum load computed from reference 3. This discrepancy is believed to be due to recent improvements in spot-welding techniques. It is felt, therefore, that a new investigation of the strength of spot-welded joints would be a worthwhile contribution.

DESIGN CURVES FOR RIVETED JOINTS

Design curves for the group A, group B, and group C joints are given in figures 20(a) to 20(c), respectively. These figures express the loads required to produce various extensions and rupture as a function of test time. The extensions are given in percentages of the nominal rivet diameter, 0.125 inch. Extensions are plotted for only a few of the joints tested at 300° F, because at this temperature the change in extension from time zero to rupture was generally quite small.

CONCLUDING REMARKS

The creep of aluminum-alloy riveted joints is considerably greater than the tensile creep of unriveted sheet and no correlation between the

two could be found. The shape of the creep curves, however, suggests that a correlation between the creep of a riveted joint and the creep of its component materials in tension, bearing, and shear may be possible.

At temperatures up to 500° F, an elastically loaded aluminum-alloy riveted joint will have a rupture time of at least 60 hours and in some cases more than several hundred hours. A rough estimate of the creep-rupture strength of a joint may be obtained by assuming the creep-rupture efficiency at the temperature in question to be equal to the room-temperature efficiency of the joint. A more accurate computation of the load required to produce creep rupture of a joint at a specific temperature in a given time is achieved by using the relation

$$P = cT^m t^n$$

where P represents the load, T represents the absolute temperature, t represents the time to rupture, and c, m, and n are constants, n depending upon the design of the joint and temperature and c and m depending solely upon the design of the joint.

The creep of spot-welded lap joints of cold-worked austenitic stainless steel at 800° F is negligible, at least up to 200 hours.

National Bureau of Standards,
Washington, D. C., August 6, 1954.

REFERENCES

1. Stickley, G. W., and Anderson, H. L.: Creep Resistance of Riveted Joints. Rep. 9-51-18, Aluminum Res. Lab., Aluminum Co. of Am., Dec. 4, 1951. (Not released for publication.)

2. Wylie, R. D., Corey, C. L., and Leyda, W. E.: The Stress Rupture Properties of Some Chromium-Nickel Stainless Steel Weld Deposits. Advance Paper No. 53-A-152, A.S.M.E., 1953.

3. Anon.: Strength of Metal Aircraft Elements. ANC-5, Munitions Board Aircraft Committee. Revised ed., June 1951.

4. Stang, A. H., and Sweetman, L. R.: Speed Control for Screw-Power Testing Machines Driven by Direct-Current Motors. Bull. No. 87, A.S.T.M. (Philadelphia), Aug. 1937, pp. 15-18.

5. Anon.: Mechanical Properties of Metals and Alloys. Circular No. C447, Nat. Bur. Standards, U. S. Govt. Printing Office, Dec. 1, 1943.

6. Jackson, L. R., Cross, H. C., and Berry, J. M.: Tensile, Fatigue, and Creep Properties of Forged Aluminum Alloys at Temperatures up to 800° F. NACA TN 1469, 1948.

7. Anon.: Steels for Elevated Temperature Service. 18566(s), Advertising Div., United States Steel Corp., 1949.

8. Vawter, F. J., Guarnieri, G. J., Yerkovich, L. A., and Salvaggi, J.: Investigation of the Compressive, Bearing, and Shear Creep-Rupture Properties of Aircraft Structural Metals and Joints at Elevated Temperatures. Rep. KB-831-M-1, Contract AF 33(616)-190, WADC and Cornell Aero. Lab., Inc., Oct. 1, 1952.

9. Vawter, F. J., Guarnieri, G. J., Yerkovich, L. A., and Salvaggi, J.: Investigation of the Compressive, Bearing, and Shear Creep-Rupture Properties of Aircraft Structural Metals and Joints at Elevated Temperatures. Rep. KB-831-M-2, Contract AF 33(616)-190, WADC and Cornell Aero. Lab., Inc., Dec. 1, 1952.

10. Vawter, F. J., Guarnieri, G. J., Yerkovich, L. A., and Salvaggi, J.: Investigation of the Compressive, Bearing, and Shear Creep-Rupture Properties of Aircraft Structural Metals and Joints at Elevated Temperatures. Rep. KB-831-M-3, Contract AF 33(616)-190, WADC and Cornell Aero. Lab., Inc., Feb. 1, 1953.

11. Doerr, D. D.: Determination of Physical Properties of Nonferrous Structural Sheet Materials at Elevated Temperatures. AF Tech. Rep. 6517, pt. 1, Contract AF 33(038)-8681, WADC and Armour Res. Foundation, Dec. 1951.

12. Dorn, J. E., and Tietz, T. E.: Creep and Stress-Rupture Investigations on Some Aluminum Alloy Sheet Metals. Proc. A.S.T.M., vol. 49, 1949, pp. 815-831.

13. Shepard, Lawrence A., Starr, C. Dean, Wiseman, Carl D., and Dorn, John E.: The Creep Properties of Metals Under Intermittent Stressing and Heating Conditions - Intermittent Stressing. WADC Tech. Rep. 53-336, pt. 1, Contract AF-33(038)-11502, WADC and Univ. of Calif., May 1954.

14. VanEcho, J. A., Page, L. C., Simmons, W. F., and Cross, H. C.: Short-Time Creep Properties of Structural Sheet Materials for Aircraft and Missiles. AF Tech. Rep. 6731, pt. 1, Contract AF 33(038)-8743, WADC and Battelle Memorial Inst., Aug. 1952.

15. Anon.: Raising the Creep Limit by Cold Working. Brown Boveri Review, vol. 33, no. 9, Sept. 1946, pp. 227-234.

SELECTED BIBLIOGRAPHY OF CREEP DATA OF AIRCRAFT

STRUCTURAL MATERIALS

Aluminum Alloys (see also refs. 6, 8, 9, 10, 12, 13, and 14):

Carlson, R. L., and Schwope, A. D.: Investigation of Compressive-Creep Properties of Aluminum Columns at Elevated Temperatures. WADC Tech. Rep. 52-251, pt. 1, Contract AF 33(038)-9542, WADC and Battelle Memorial Inst., Sept. 1952.

Flanigan, A. E., Tedsen, L. F., and Dorn, J. E.: Stress Rupture and Creep Tests on Aluminum-Alloy Sheet at Elevated Temperatures. Trans. Am. Inst. Min. and Metall. Eng., vol. 171, 1947, pp. 213-244.

Kennedy, R. R.: Creep Characteristics of Aluminum Alloys. Proc. A.S.T.M., vol. 35, pt. II, 1935, pp. 218-231.

Marin, J., Faupel, J. H., and Hu, L. W.: Combined Tension-Torsion Creep-Time Relations for Aluminum Alloy 2S-O. Proc. A.S.T.M., vol. 50, 1950, pp. 1054-1070.

McKeown, J., and Lushey, R. D. S.: Creep Properties of Some Aluminum Alloys at Temperatures up to 300° C. Metallurgia, vol. 43, no. 255, Jan. 1951, pp. 15-19.

Sherby, O. D., and Dorn, J. E.: The Creep Properties of Two Tempers of 63S Extruded Aluminum Alloy. Proc. A.S.T.M., vol. 51, 1951, pp. 945-953.

Sherby, O. D., and Dorn, J. E.: Effect of Annealing on the Creep Properties of 2S-O Aluminum Alloy. Proc. A.S.T.M., vol. 51, 1951, pp. 954-963.

Sherby, O. D., and Dorn, J. E.: The Effect of Cold Rolling on the Creep Properties of Several Aluminum Alloys. Trans. A.S.M., vol. 43, 1951, pp. 611-634.

Sherby, O. D., Tietz, T. E., and Dorn, J. E.: The Creep Properties of Some Forged and Cast Aluminum Alloys. Proc. A.S.T.M., vol. 51, 1951, pp. 964-976.

Wyman, L. L.: High Temperature Properties of Light Alloys (NA-137). I - Aluminum. OSRD No. 3607, Serial No. M-251, War Metall. Div., NDRC, Apr. 15, 1944.

Magnesium Alloys (see also ref. 14):

Johnson, A. E.: The Creep of a Nominally Isotropic Magnesium Alloy at Normal and Elevated Temperatures Under Complex Stress Systems. Metallurgia, vol. 42, no. 252, Oct. 1950, pp. 249-262.

Johnson, A. E., Tapsell, H. J., and Conway, H. D.: Creep Tests on Some Cast Magnesium Alloys. R. & M. No. 2675, British A.R.C., 1951.

Leontis, T. E., and Murphy, J. P.: Properties of Cerium-Containing Magnesium Alloys at Room and Elevated Temperatures. Trans. Am. Inst. Min. and Metall. Eng., vol. 166, 1946, pp. 295-326.

Mellor, G. A., and Ridley, R. W.: The Creep Strength at 200° C of Some Magnesium Alloys Containing Cerium. The Jour. Inst. Metals, vol. 75, pt. 8, Apr. 1949, pp. 679-692.

Moore, A. A., and McDonald, J. C.: Tensile and Creep Strengths of Some Magnesium Base Alloys at Elevated Temperature. Symposium on Materials for Gas Turbines, A.S.T.M., 1946, pp. 180-199.

Titanium and Titanium Alloys (see also refs. 8, 9, 10, and 13):

Adenstedt, H.: Creep of Titanium at Room Temperature. Metal Progress, vol. 56, no. 5, Nov. 1949, pp. 658-660.

Anon.: Creep of Commercially Pure Titanium. Rem-Cru Titanium Rev., vol. 1, no. 3, Jan. 1953, pp. 5-8.

Anon.: Handbook on Titanium Metal. Seventh ed., Titanium Metals Corp. of Am. (New York), Aug. 1, 1953.

Cuff, Frank B., Jr., and Grant, Nicholas J.: Stress-Rupture Characteristics of Unalloyed Titanium Plotted. The Iron Age, vol. 170, no. 21, Nov. 20, 1952, pp. 134-139.

Gluck, J. V., and Freeman, J. W.: A Study of Creep of Titanium and Two of Its Alloys. Prog. Rep. 13, Contract AF 33(038)-14111, WADC and Eng. Res. Inst., Univ. of Mich., Dec. 1953.

Kiessel, W. R., and Sinnott, M. J.: Creep Properties of Commercially Pure Titanium. Jour. Metals, vol. 5, no. 2, sec. 2 (Trans. Supp.), Feb. 1953, pp. 331-338.

Alloy Steels (see also refs. 8, 9, 10, and 14):

Summaries of significant literature on creep data of alloy steels may be found in publications of the various steel companies and the American Society for Testing Materials. Recent investigations which may not have been thus summarized include the following reports:

Dulis, E. J., and Smith, G. V.: Creep and Creep-Rupture of Some Ferritic Steels Containing 5 Per Cent to 17 Per Cent Chromium. Preprint 66, A.S.T.M., 1953.

Freeman, J. W., Comstock, G. F., and White, A. E.: Rupture and Creep Characteristics of Titanium-Stabilized Stainless Steel at 1100 to 1300 F. Trans. A.S.M.E., vol. 74, no. 5, July 1952, pp. 793-801.

Rush, A. I., and Freeman, J. W.: Statistical Evaluation of the Creep-Rupture Properties of Four Heat-Resistant Alloys in Sheet Form. Preprint 82, A.S.T.M., 1954.

Smith, G. V., Dulis, E. J., and Houston, E. G.: Creep and Rupture of Several Chromium-Nickel Austenitic Stainless Steels. Trans. A.S.M., vol. 42, 1950, pp. 935-978.

Smith, G. V., and Seens, W. B.: Short-Time Tension and Creep Rupture Properties of Hardened 1040, 4340, and Ni-Cr-Mo-V Steels up to 1000 F. Preprint 78, A.S.T.M., 1954.

TABLE 1.- DESCRIPTION OF SPECIMENS

[See also fig. 1]

Group	Sheet material	Fastener	Doubler material	Edge distance, e
A	0.032-in. alclad 75S-T6 aluminum-alloy sheet	1/8-in. 24S aluminum-alloy round-head rivets	1/8-in. 24S-T4 aluminum-alloy strip	[a]2.0D
B	0.032-in. alclad 24S-T3 aluminum-alloy sheet	1/8-in. 24S-T31 aluminum-alloy universal-head rivets	1/8-in. 24S-T4 aluminum-alloy strip	[a]2.0D
C	0.032-in. alclad 24S-T3 aluminum-alloy sheet	1/8-in. 24S-T31 aluminum-alloy universal-head rivets	1/8-in. 24S-T4 aluminum-alloy strip	[a]2.5D
S	0.037-in. stainless-steel strip, type 301, 1/4 hard, 2B finish	1/4-in. spotwelds	3/32-in. stainless-steel sheet, type 302, annealed, 2B finish	1/4 in.

[a]D = Rivet diameter = 1/8 in.

TABLE 2.- RESULTS OF DOUBLE SHEAR TESTS OF

RIVETS AT ROOM TEMPERATURE

Rivet (a)	Maximum load, lb	Ultimate shear stress, psi
[b]24S-T31	1,060	43,200
[b]24S-T31	1,040	42,400
[b]24S-T31	1,020	41,600
(Average)	1,040	42,400
24S	482	19,600
24S	487	19,800
24S	484	19,700
(Average)	484	19,700

[a]For full description, see table 1.

[b]Temper is actually -T4 before driving.

TABLE 3.- RESULTS OF TENSILE TESTS OF JOINTS

AT ROOM TEMPERATURE

Group	Test	Maximum load, lb	Computed strength of unriveted sheet, lb	Efficiency, percent
A	RA-S	774	3,600	22
B	RB-S	1,680	3,000	56
C	RC-S	1,750	3,000	58
S	RS-S	6,500	6,900	94

TABLE 4.- RESULTS OF CREEP-RUPTURE TESTS

Group	Specimen	Test load, lb	Average test temperature, °F	Actual thermal expansion, in.	Initial extension, in.	Time to rupture, hr
A	3A-7.1	710	305	0.0031	(a)	0
	3A-6.3	630	298	.0033	0.0122	1.72
	3A-6	600	301	.0034	.0067	67.8
	Average		301	.0033		
A	4A-4	400	403	.0054	.0031	.8
	4A-3.5	350	403	.0054	.0025	4.35
	4A-3.1	310	404	.0053	.0022	10.8
	4A-2.75	275	403	.0054	.0016	63.6
	Average		403	.0054		
B	3B-15	1,500	306	.0035	(a)	0
	3B-13.5	1,350	300	.0035	.0231	7.87
	3B-12.5	1,250	300	.0040	.0181	17.6
	3B-10.5	1,050	302	.0030	.0114	43.1
	3B-10.3	1,030	299	.0033	.0088	164.4
	3B- 8.9	890	302	.0037	.0073	(b)
	Average		302	.0035		
B	4B-8.7	870	398	.0052	.0072	2.25
	4B-7.1	710	403	.0054	.0054	12.0
	4B-5.9	590	396	.0053	.0043	82.9
	4B-3.9	390	399	.0054	.0024	(c)
	Average		399	.0053		
B	5B-7.7	770	498	.0068	(a)	0
	5B-5	500	502	.0069	.0060	2.19
	5B-4	400	489	(d)	.0038	(e)
	5B-3.4	340	500	.0066	.0024	31.2
	Average		497	.0068		
C	4C-8.7	870	400	.0050	.0061	9.19
	4C-6.8	680	401	.0050	.0039	51.0
	Average		400	.0050		
S	8S-42	4,200	806	.0086	(a)	0
	8S-41	4,100	803	.0091	.0667	(f)
	8S-38	3,800	804	.0088	.0324	(g)
	Average		804	.0088		

[a]Specimen fractured before initial extension could be measured.

[b]Test discontinued after 169.8 hr.

[c]Test discontinued after 237.8 hr.

[d]Not determined.

[e]Test inadvertently discontinued after 6.0 hr.

[f]Test discontinued after 175.5 hr.

[g]Test discontinued after 165.2 hr.

TABLE 5.- CONSTANTS FOR EQUATIONS (3), (4), AND (5)

Group	Temperature, °F	b	n	c	m
A	300	634	-0.0134	9.55×10^{13}	-3.88
A	400	392	-.0855	9.55×10^{13}	-3.88
B	300	1,620	-.0894	2.82×10^{16}	-4.59
B	400	940	-.1093	2.82×10^{16}	-4.59
B	500	561	-.1453	2.82×10^{16}	-4.59
C	400	1,200	-.1436	(a)	(a)

[a]Insufficient tests to determine.

TABLE 6.- CREEP-RUPTURE EFFICIENCY OF RIVETED JOINTS

Joint	Creep-rupture efficiency, percent	Deviation, percent (a)
3A-7.1	26	18
3A-6.3	26	18
3A-6	32	45
4A-4	28	27
3B-15	56	0
3B-13.5	49	-12
3B-12.5	46	-18
3B-10.5	40	-29
3B-10.3	43	-23
4B-8.7	46	-18
4B-7.1	44	-21
4B-5.9	46	-18
5B-7.7	53	-5
5B-5	52	-7
4C-8.7	53	-8
4C-6.8	50	-14

[a]$\text{Deviation} = \dfrac{\text{Creep-rupture efficiency} - \text{Room-temperature efficiency}}{\text{Creep-rupture efficiency}}$.

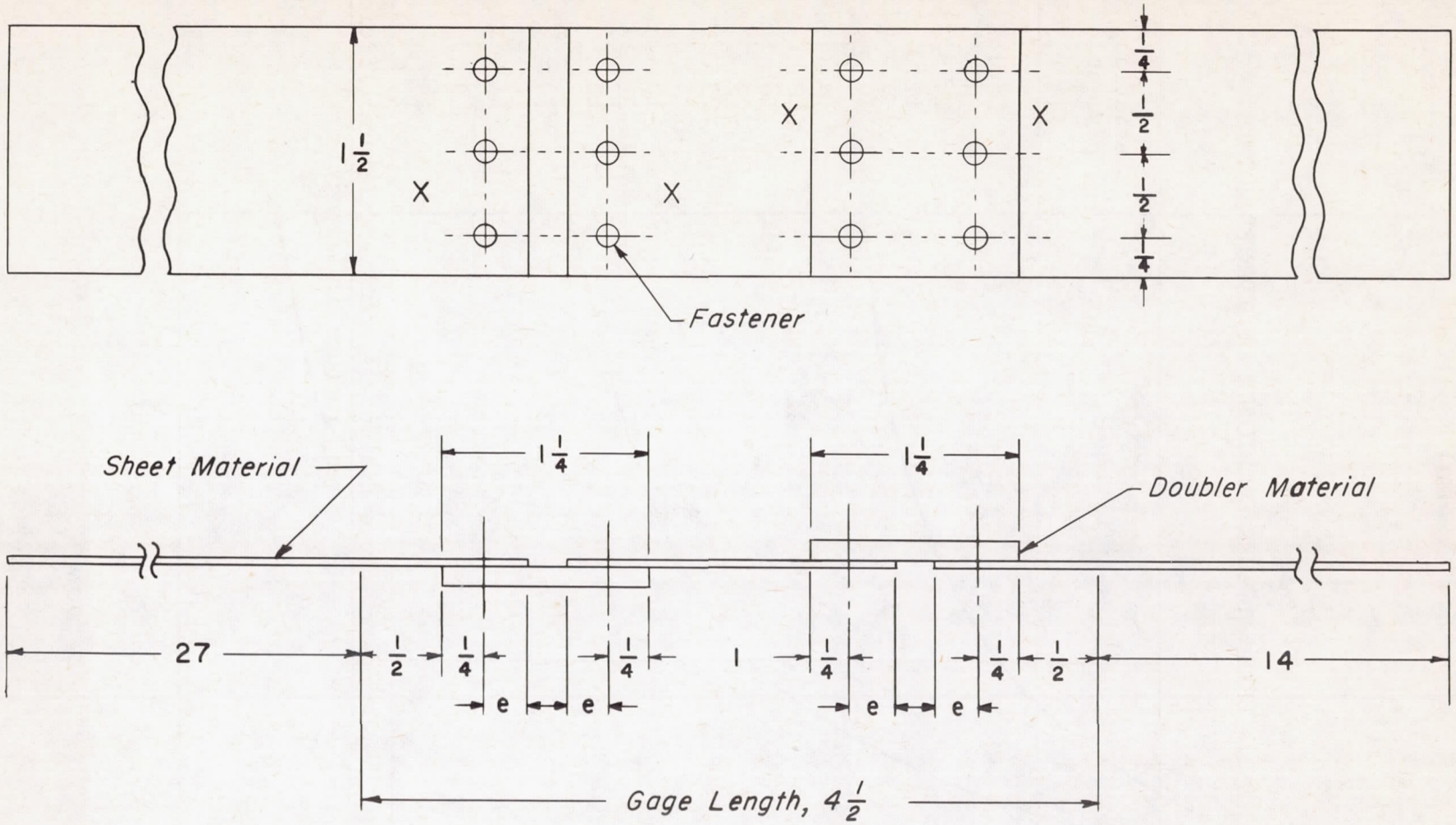

Figure 1.- Dimensions of specimens. All dimensions are in inches. × indicates location of thermocouple. See also table 1.

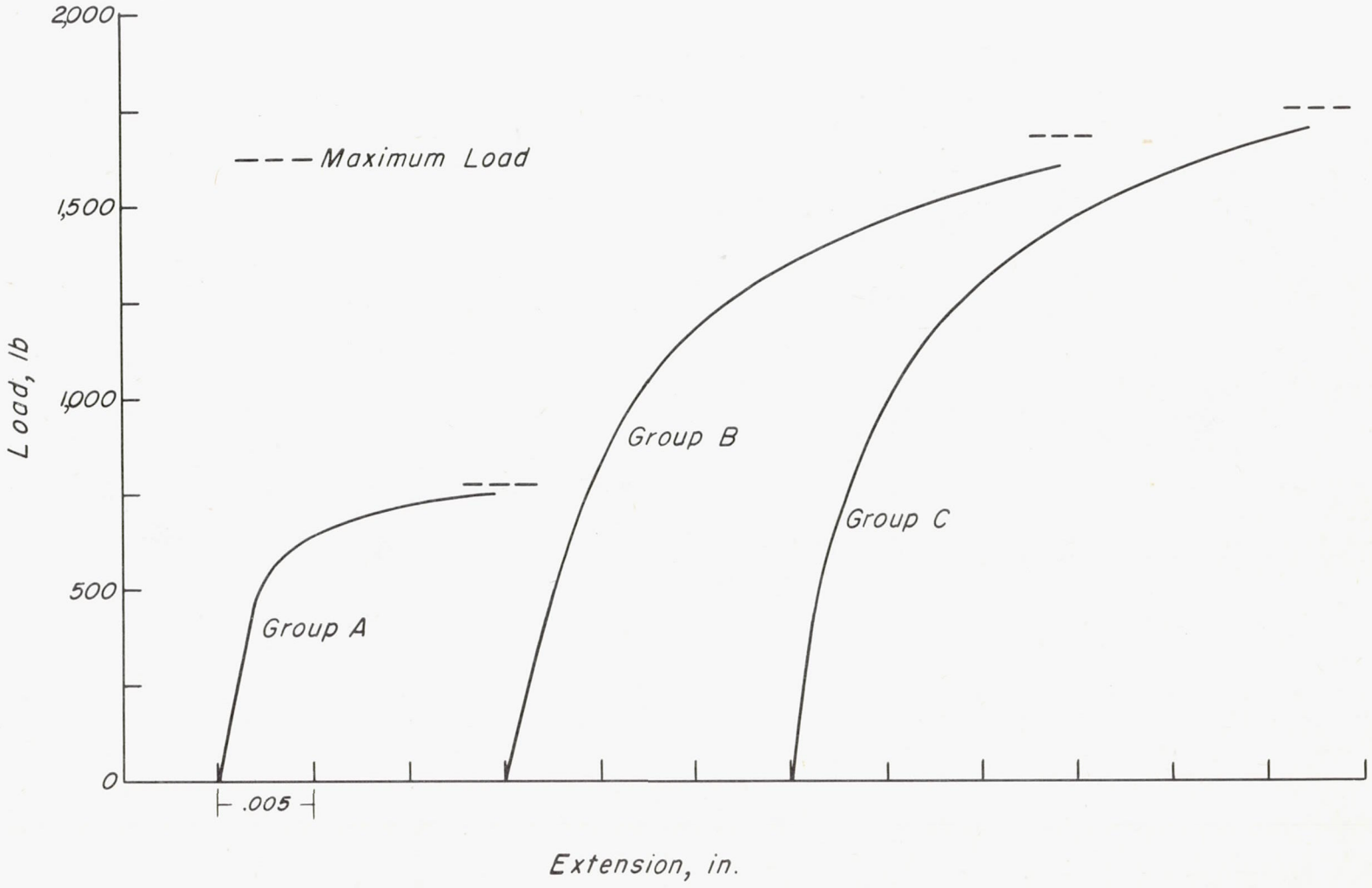

(a) Riveted aluminum-alloy joints.

Figure 2.- Load-extension curves at room temperature.

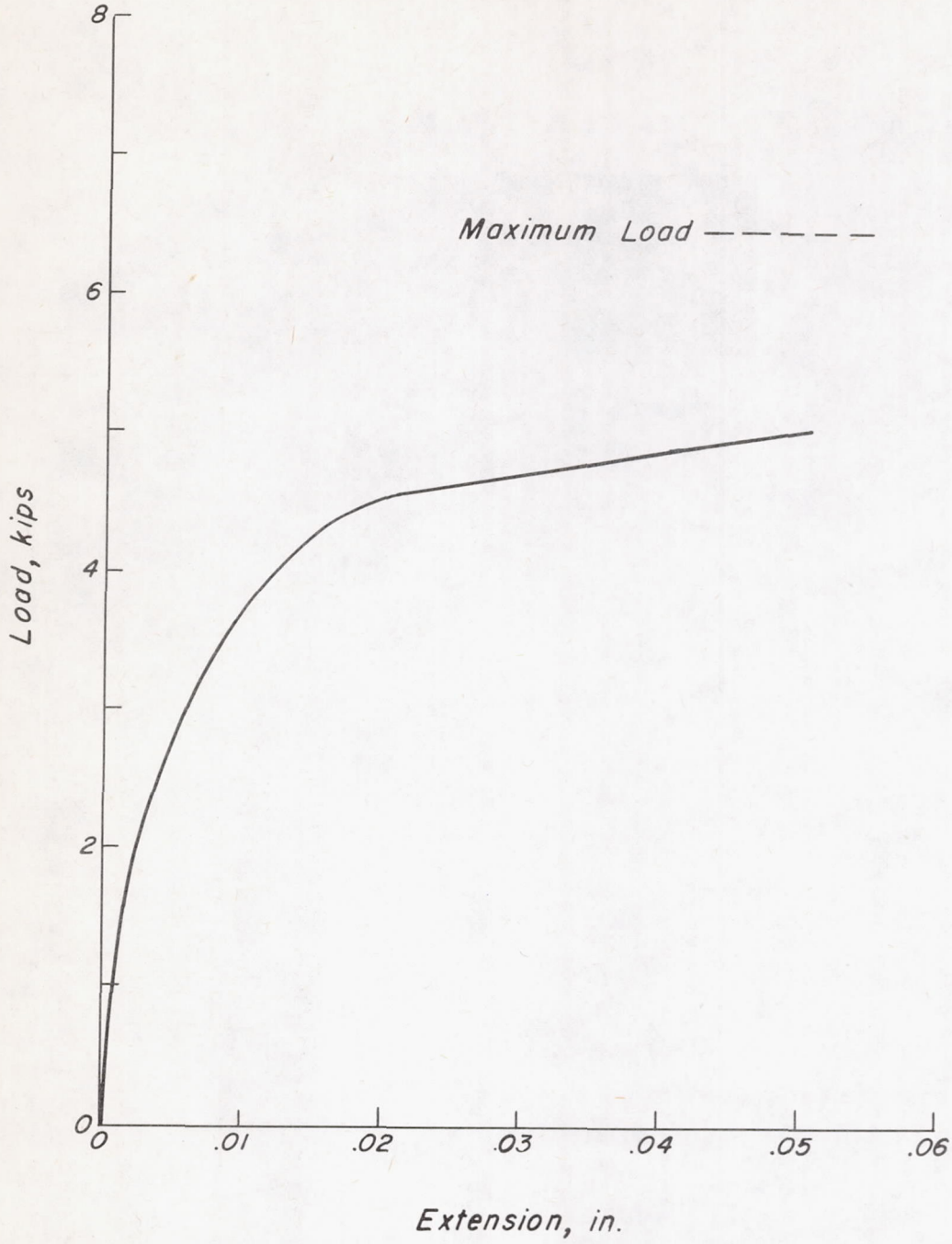

(b) Spot-welded stainless-steel joint.

Figure 2.- Concluded.

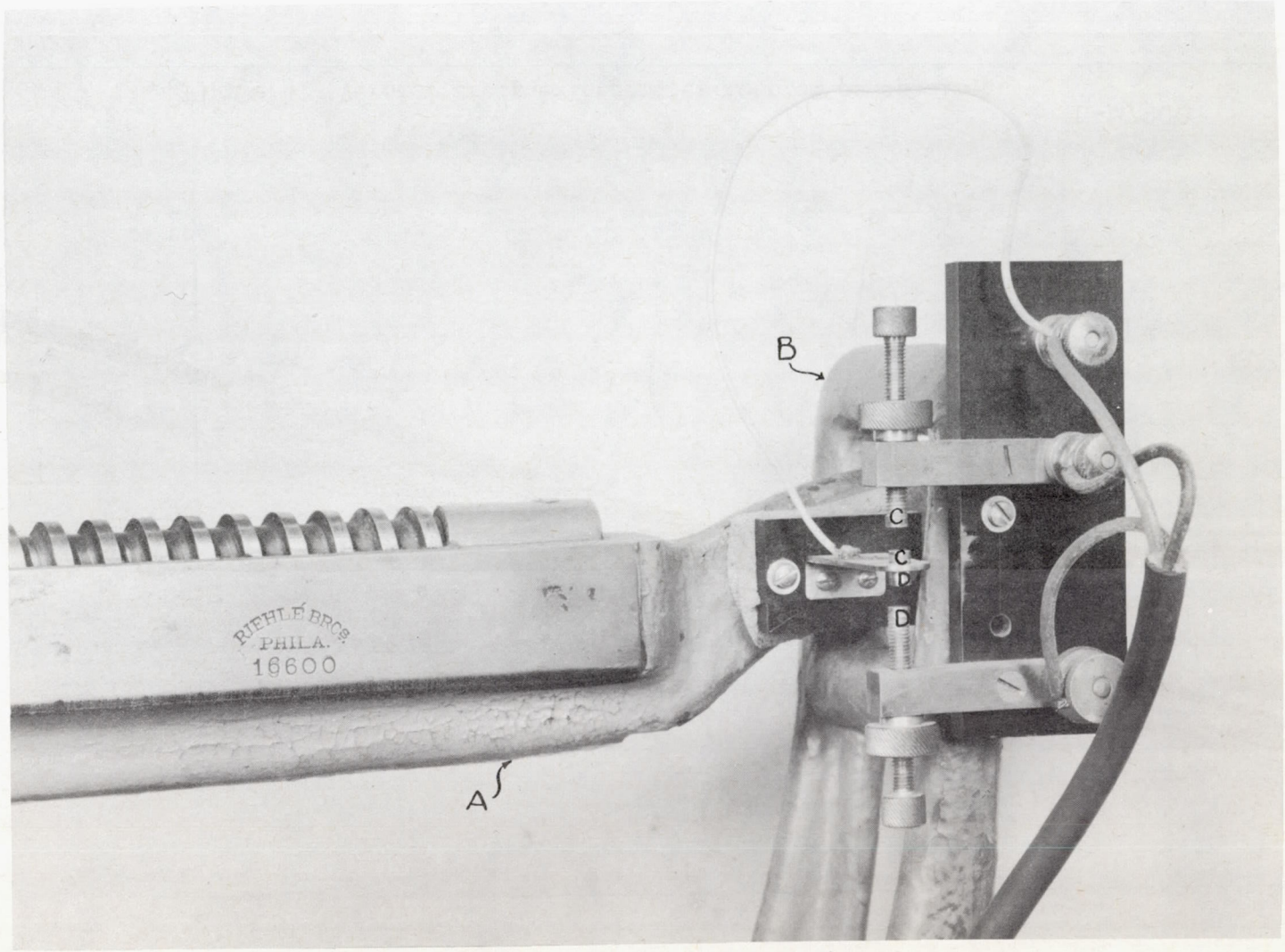

L-87899

Figure 3.- Electrical contacts for load-maintaining circuit.

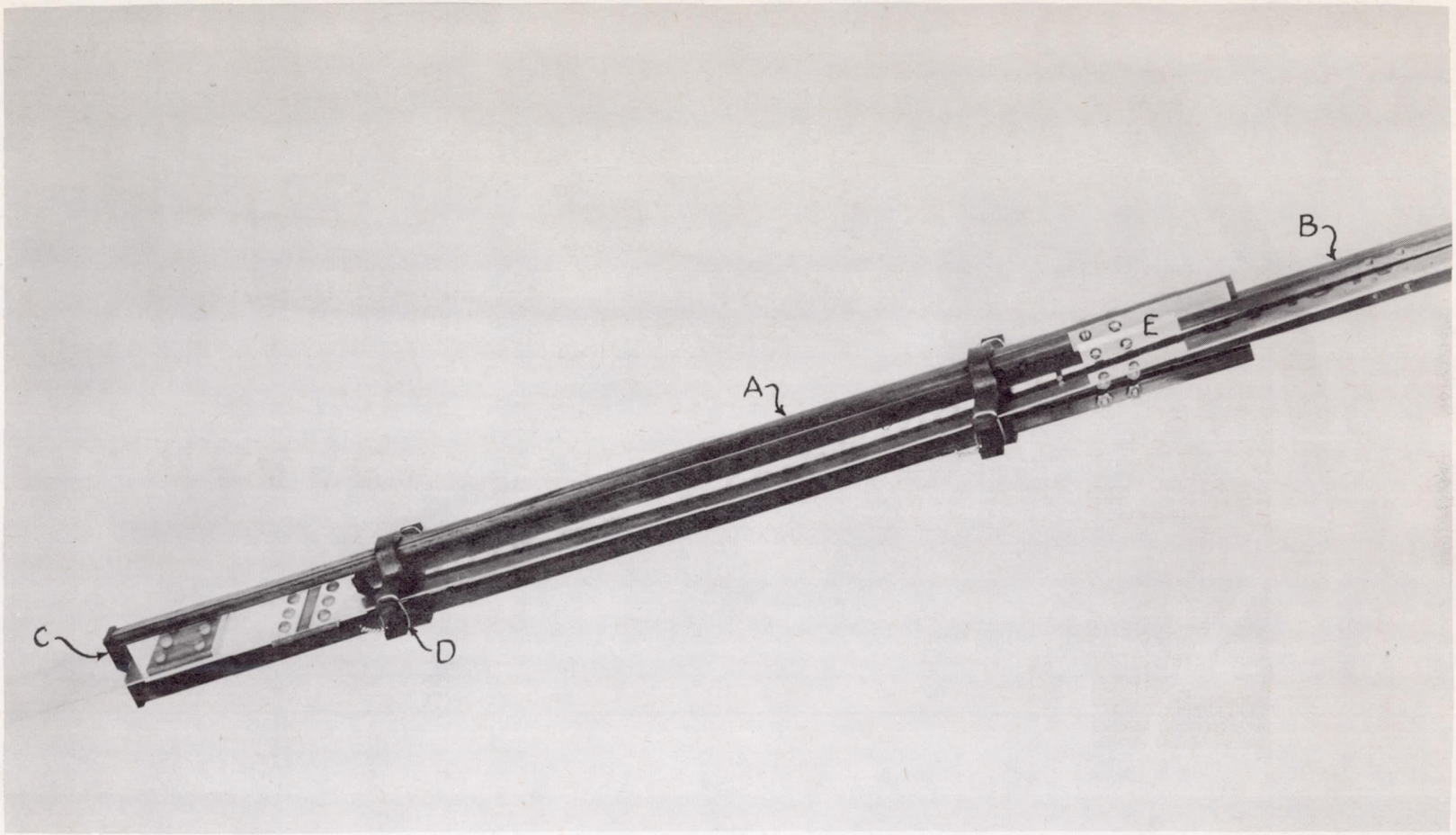

L-87900

Figure 4.- Vernier creep extensometer mounted on specimen.

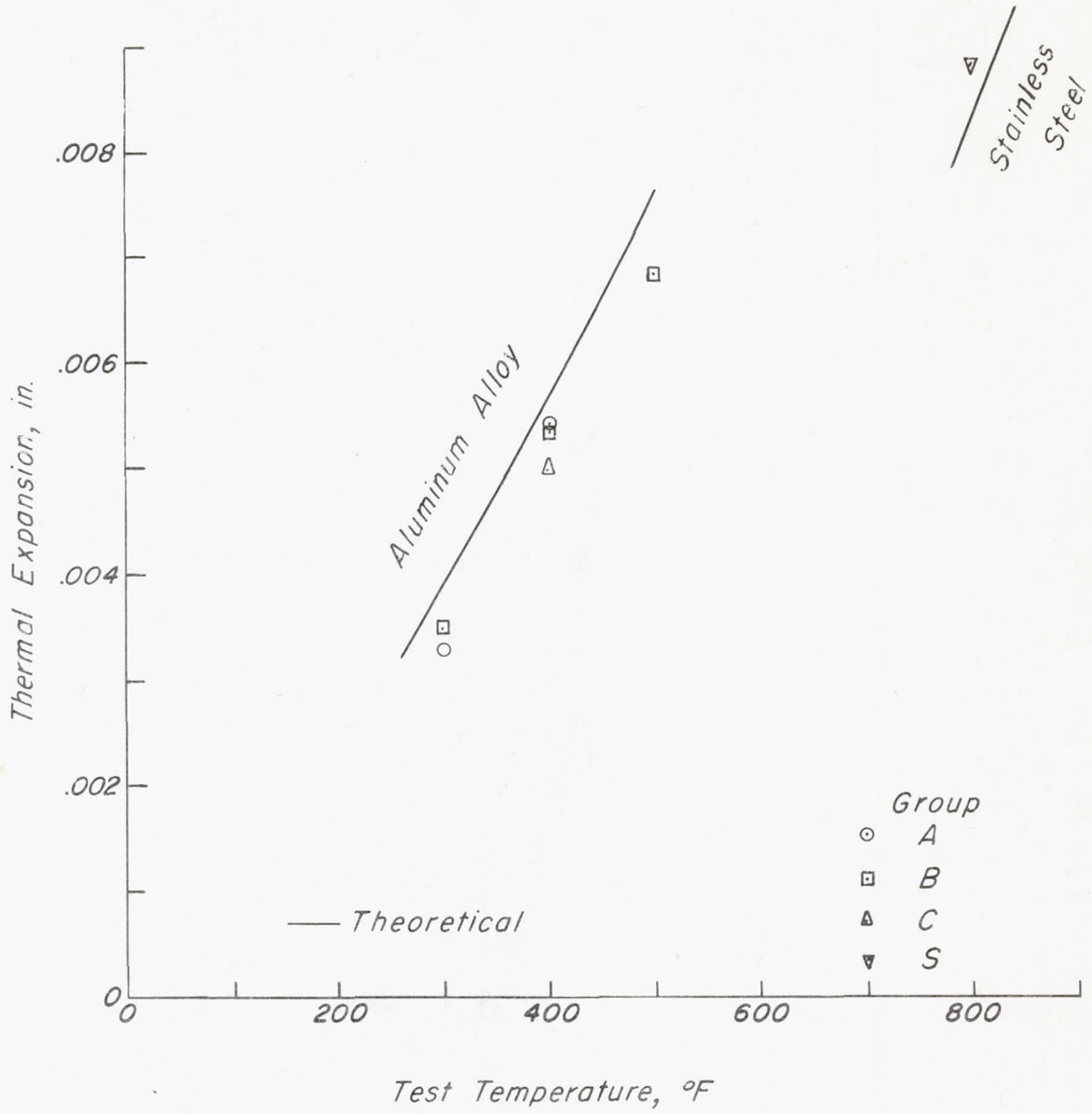

Figure 5.- Thermal expansion of joints.

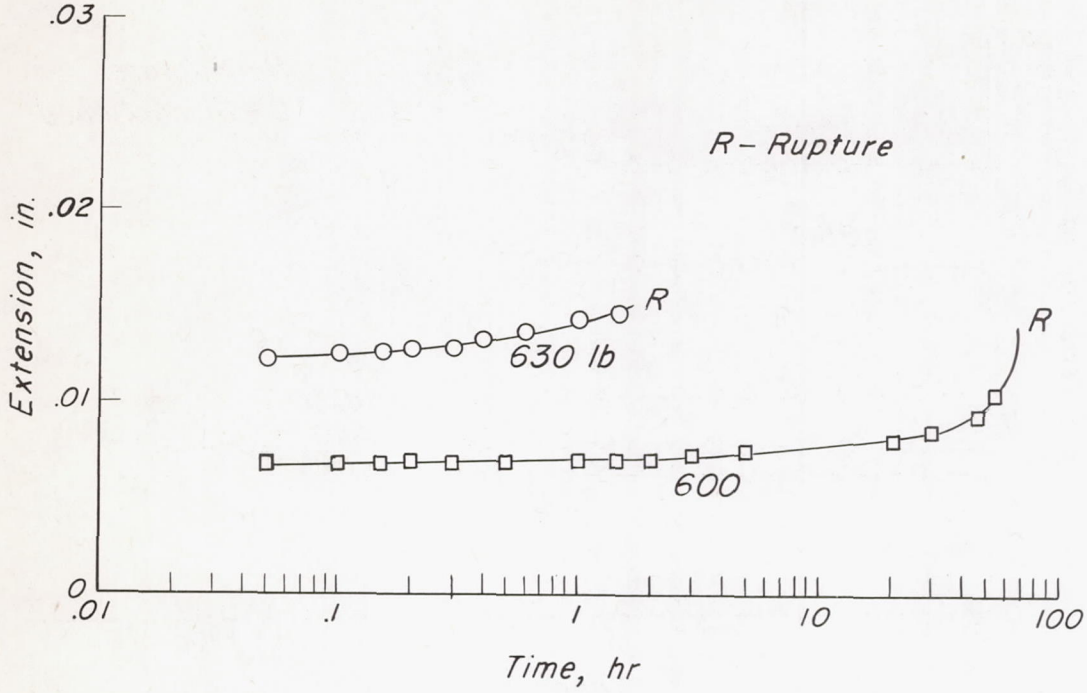

(a) Group A.

Figure 6.- Creep curves of joints at 300° F.

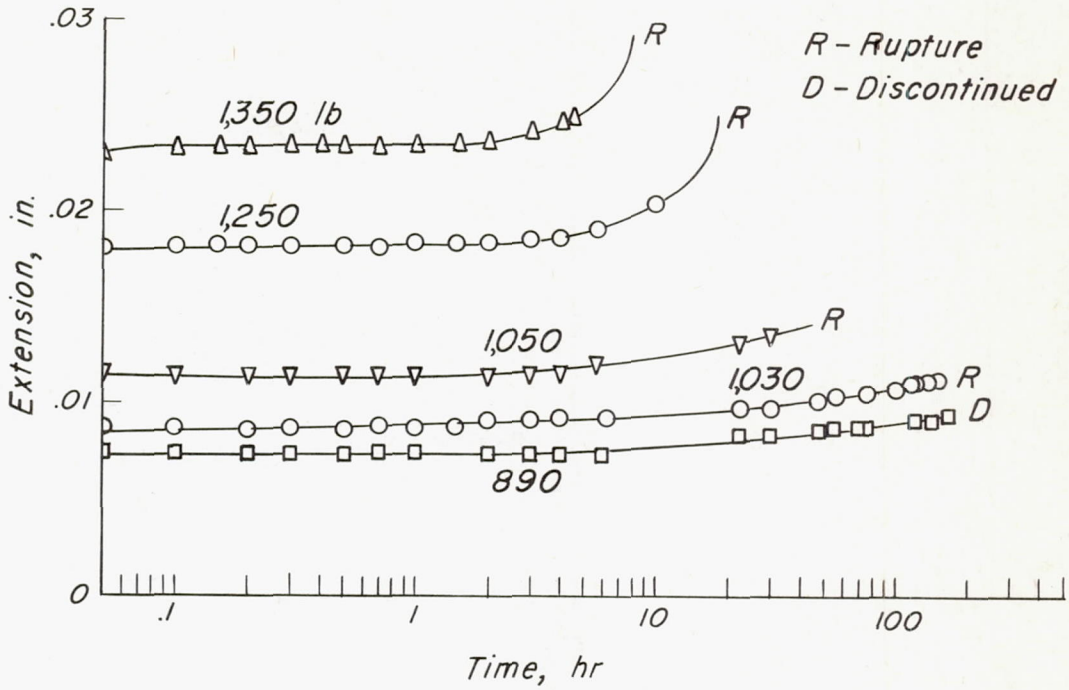

(b) Group B.

Figure 6.- Concluded.

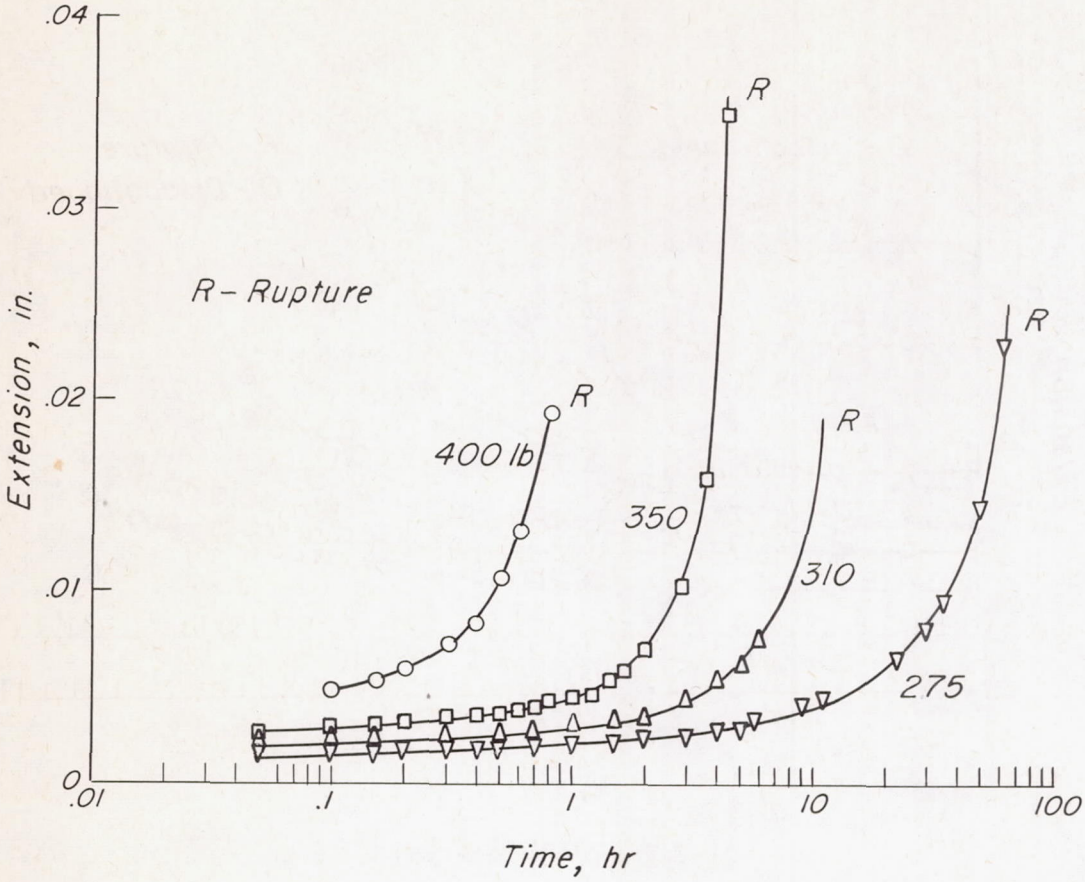

(a) Group A.

Figure 7.- Creep curves of joints at 400° F.

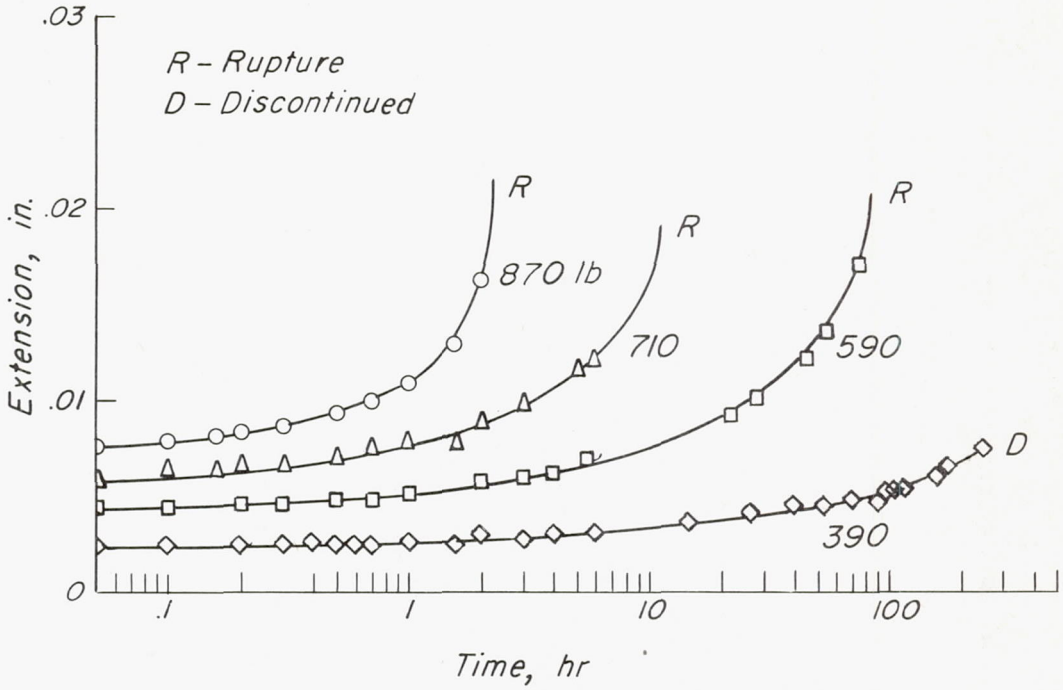

(b) Group B.

Figure 7.- Continued.

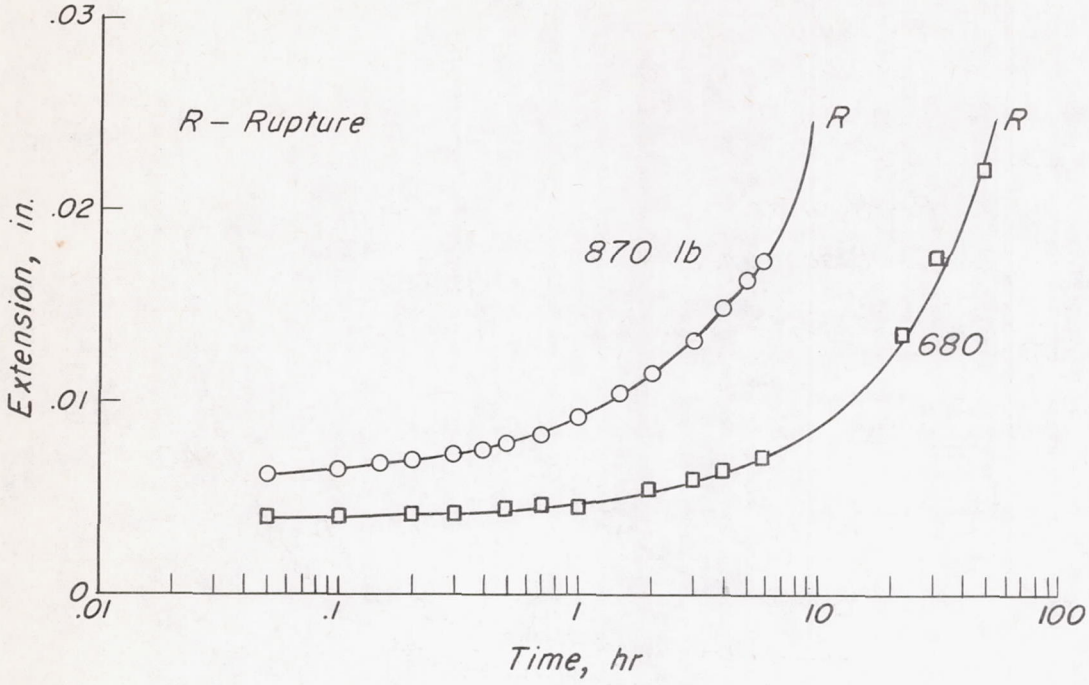

(c) Group C.

Figure 7.- Concluded.

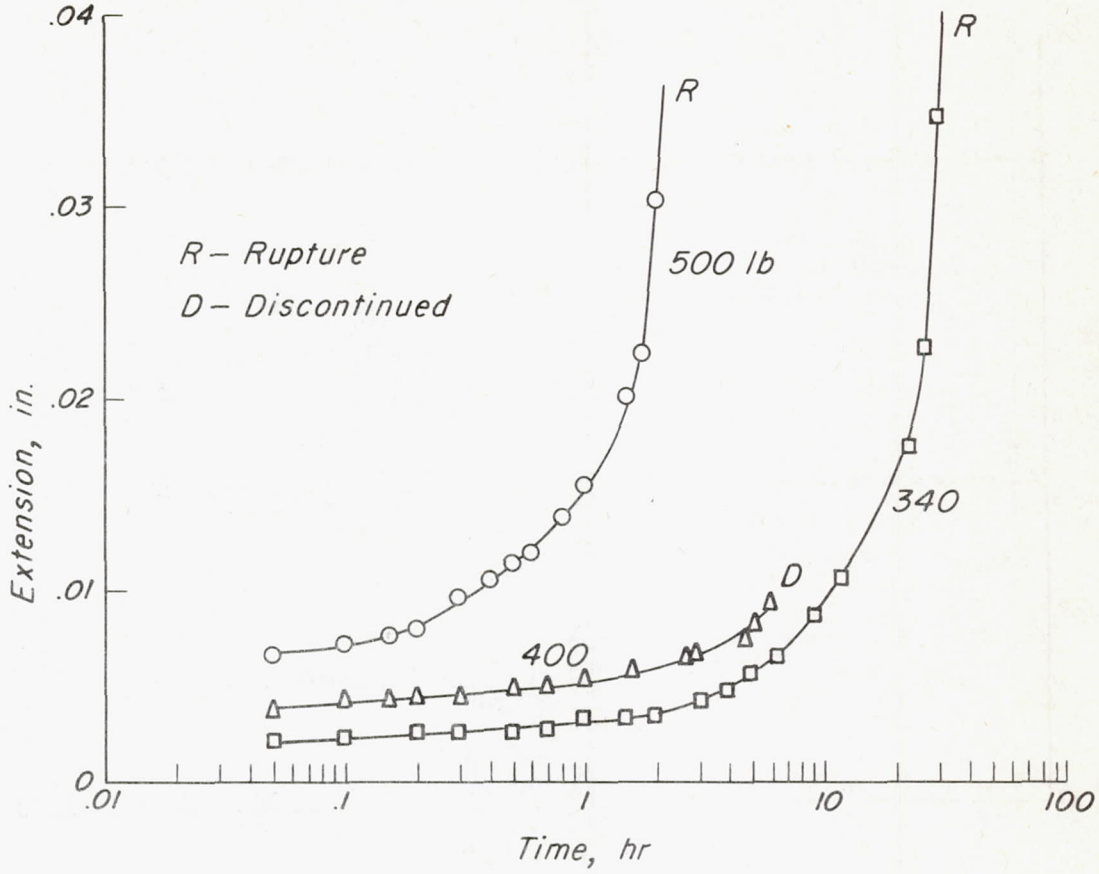

Figure 8.- Creep curves of group B joints at 500° F.

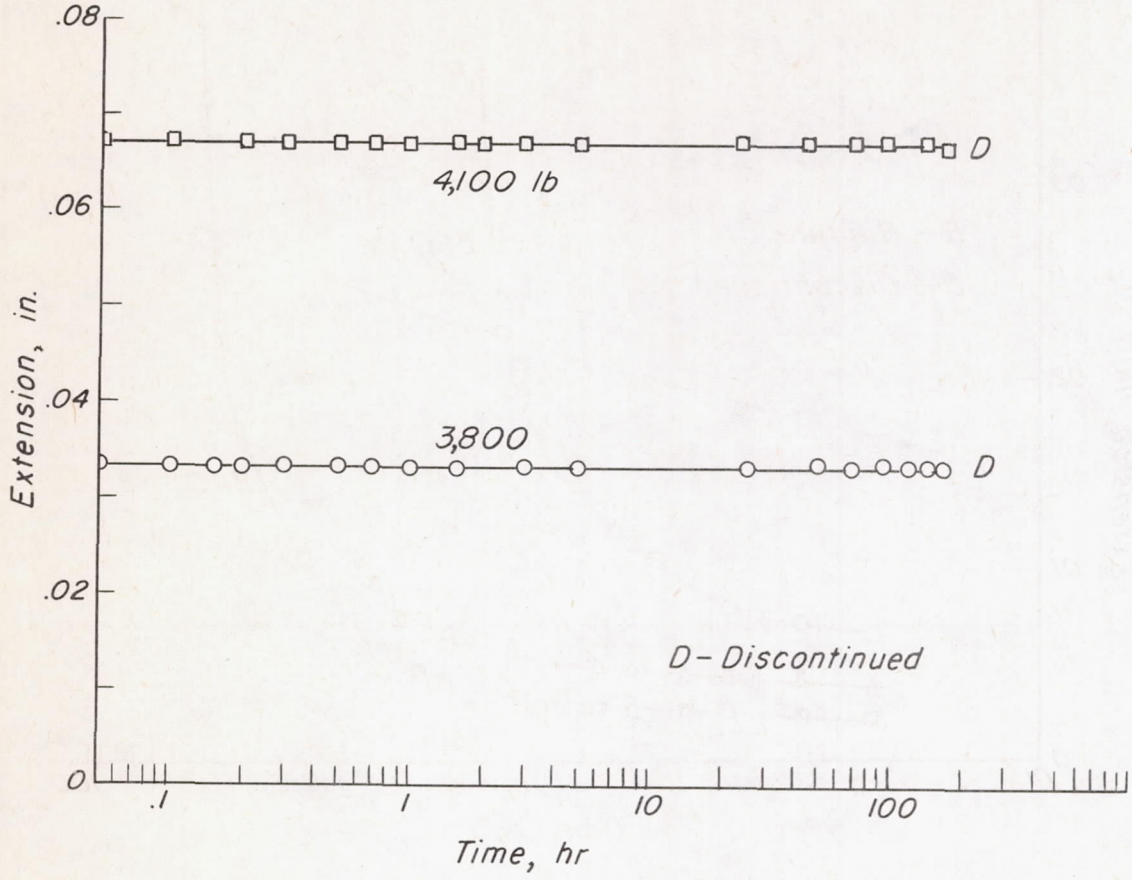

Figure 9.- Creep curves of group S joints at 800° F.

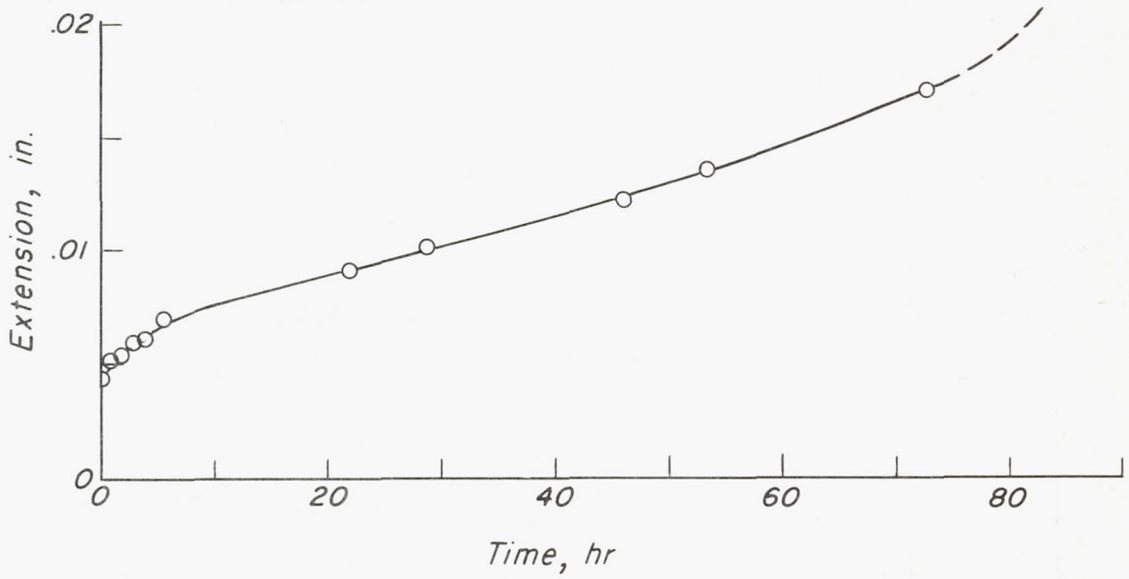

Figure 10.- Creep curve of group B joint at 590 pounds and 400° F.

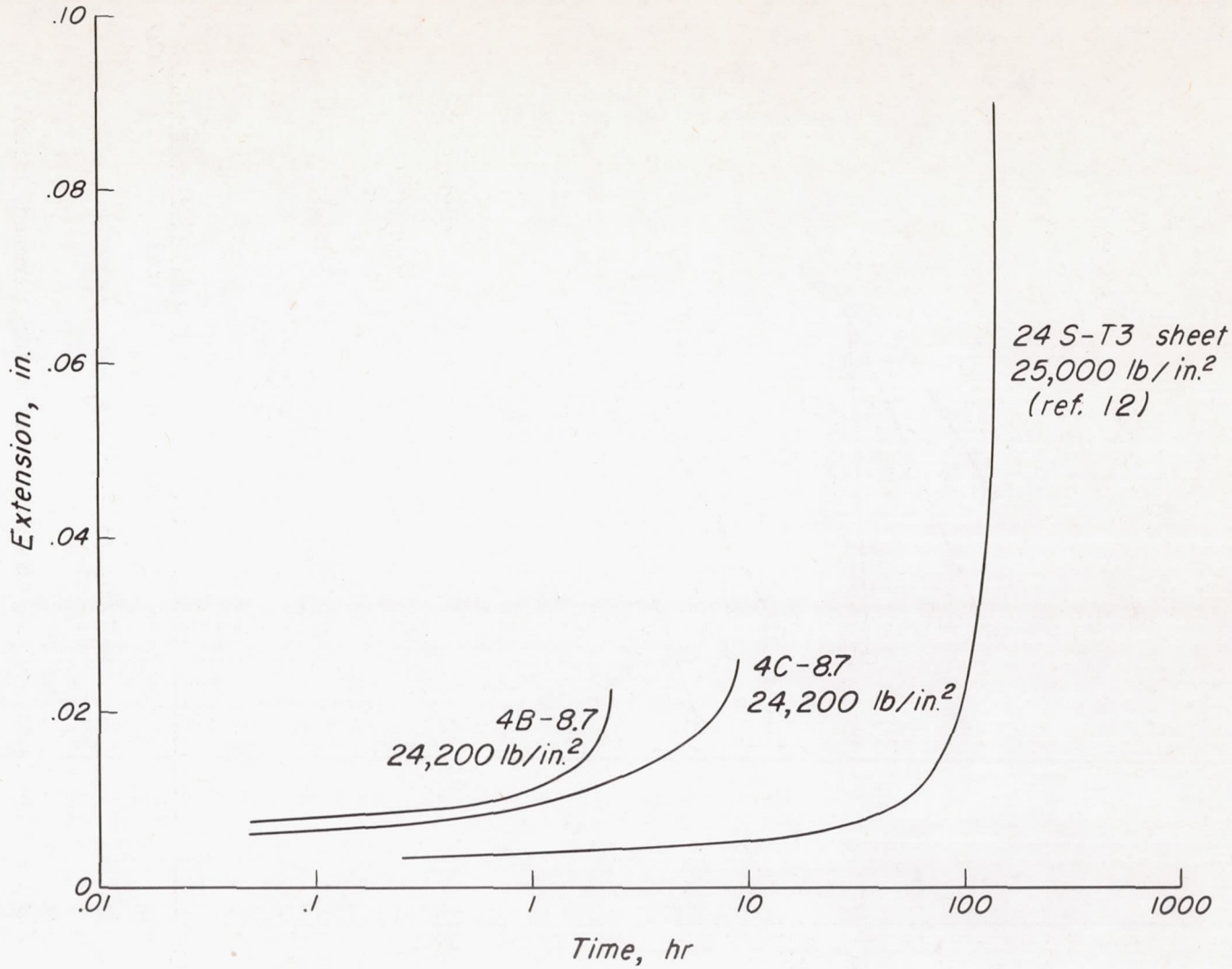

Figure 11.- Comparison of creep curves at 400° F of riveted joints and plain sheet under same net tensile stress.

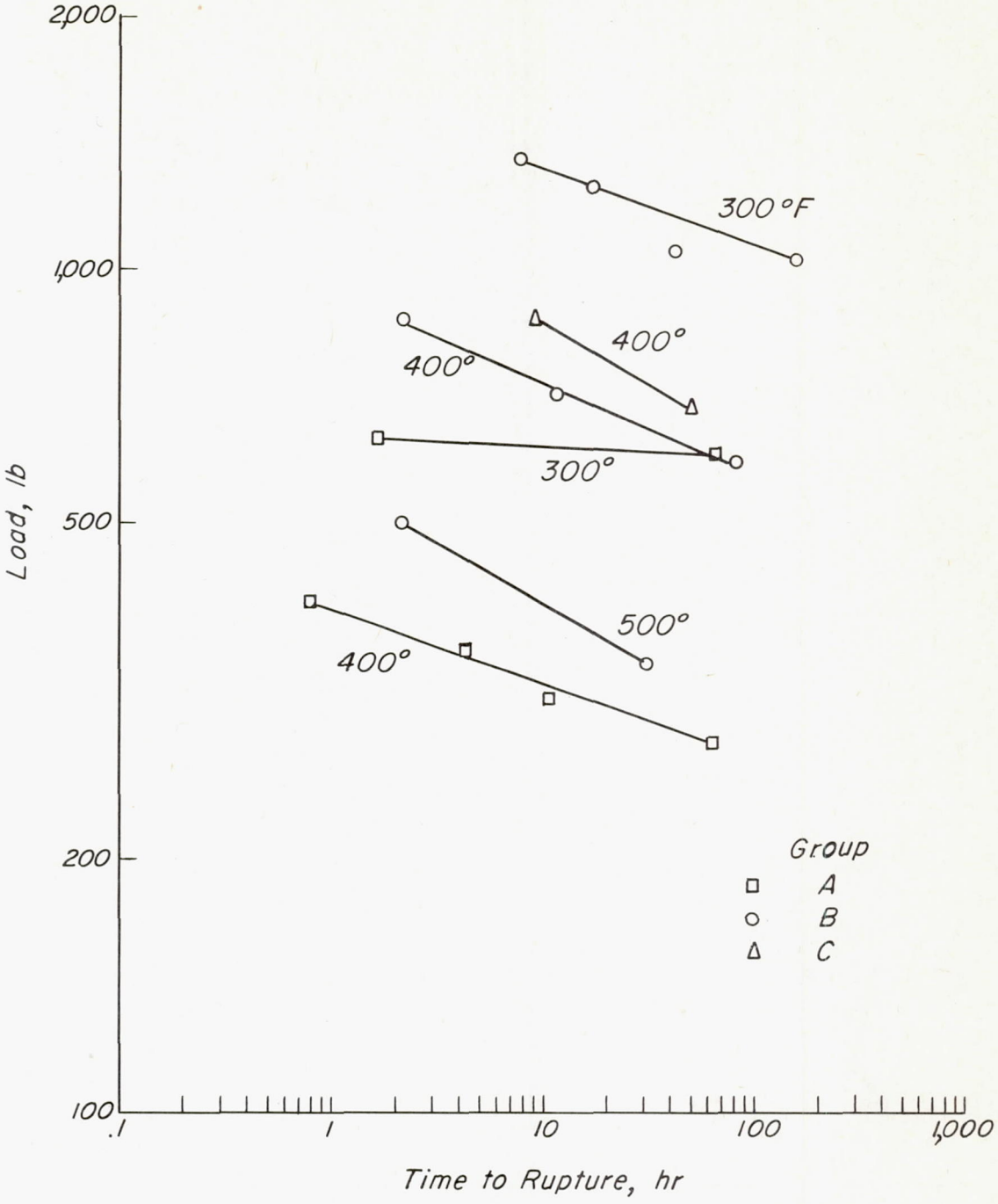

Figure 12.- Load versus time to rupture for riveted joints.

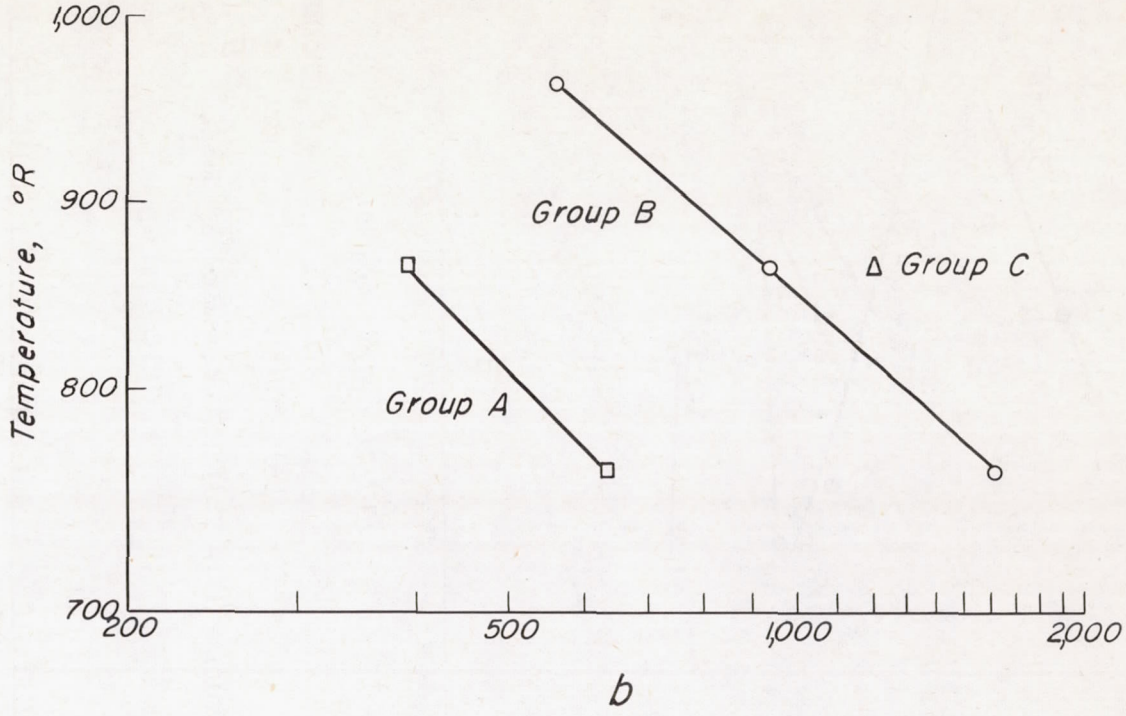

Figure 13.- Constant b, equation (3), as a function of absolute temperature.

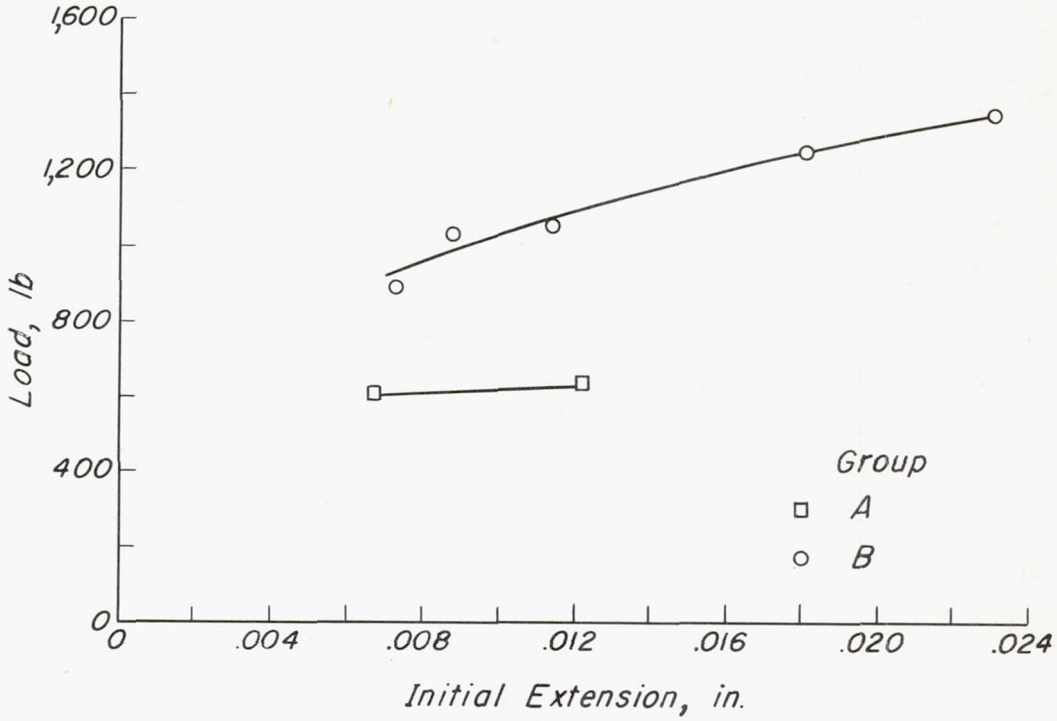

(a) 300° F.

Figure 14.- Initial extension of joints.

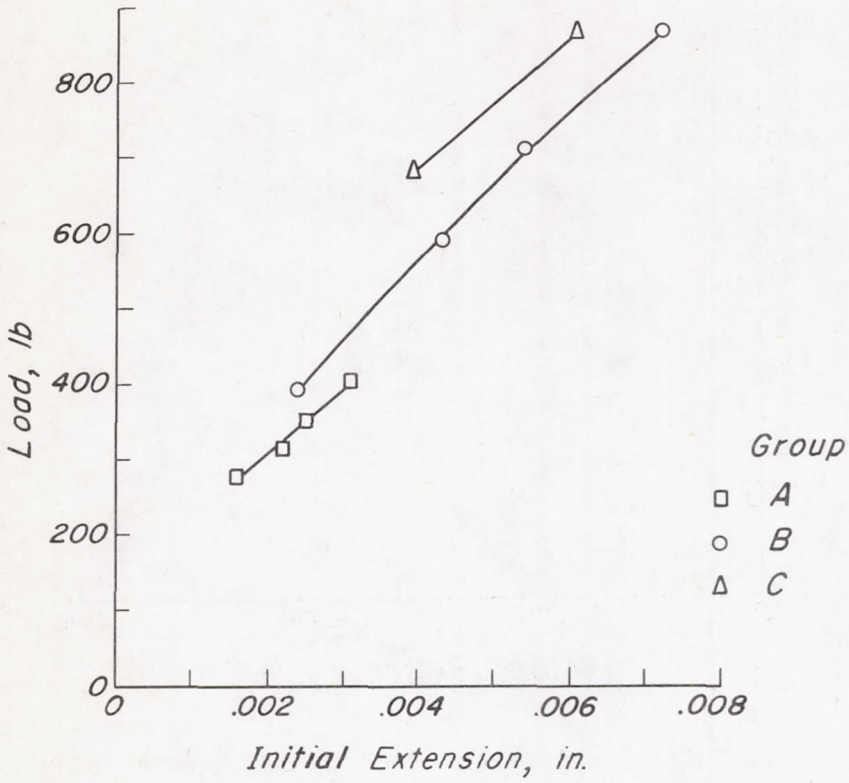

(b) 400° F.

Figure 14.- Concluded.

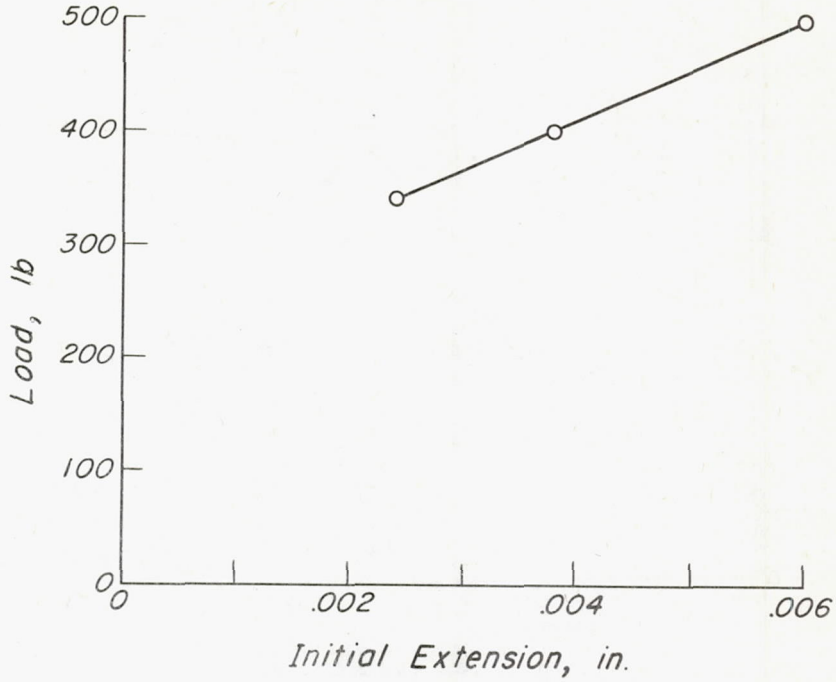

Figure 15.- Initial extension of group B joints at 500° F.

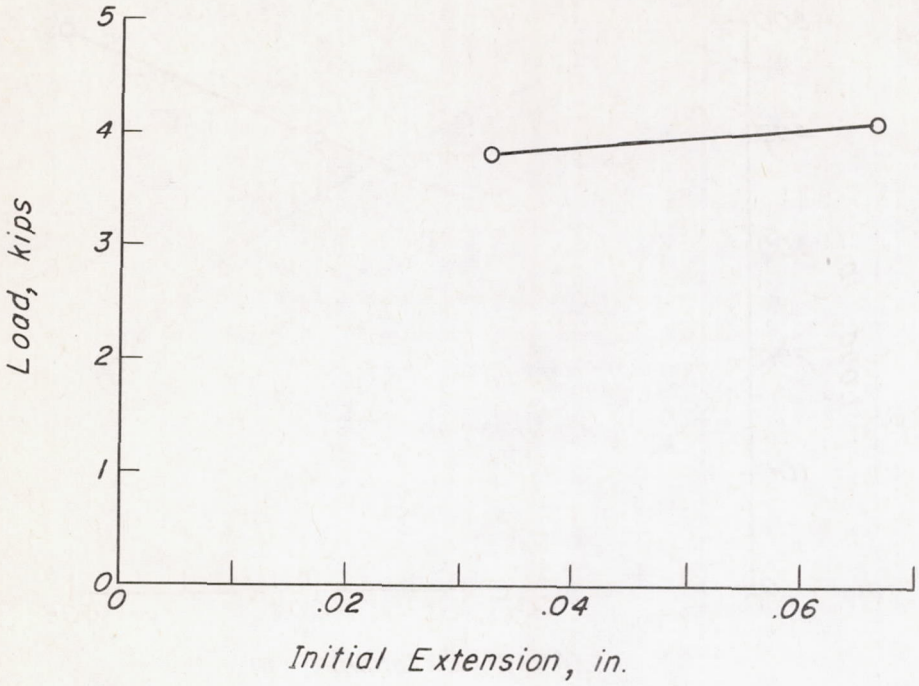

Figure 16.- Initial extension of group S joints at 800° F.

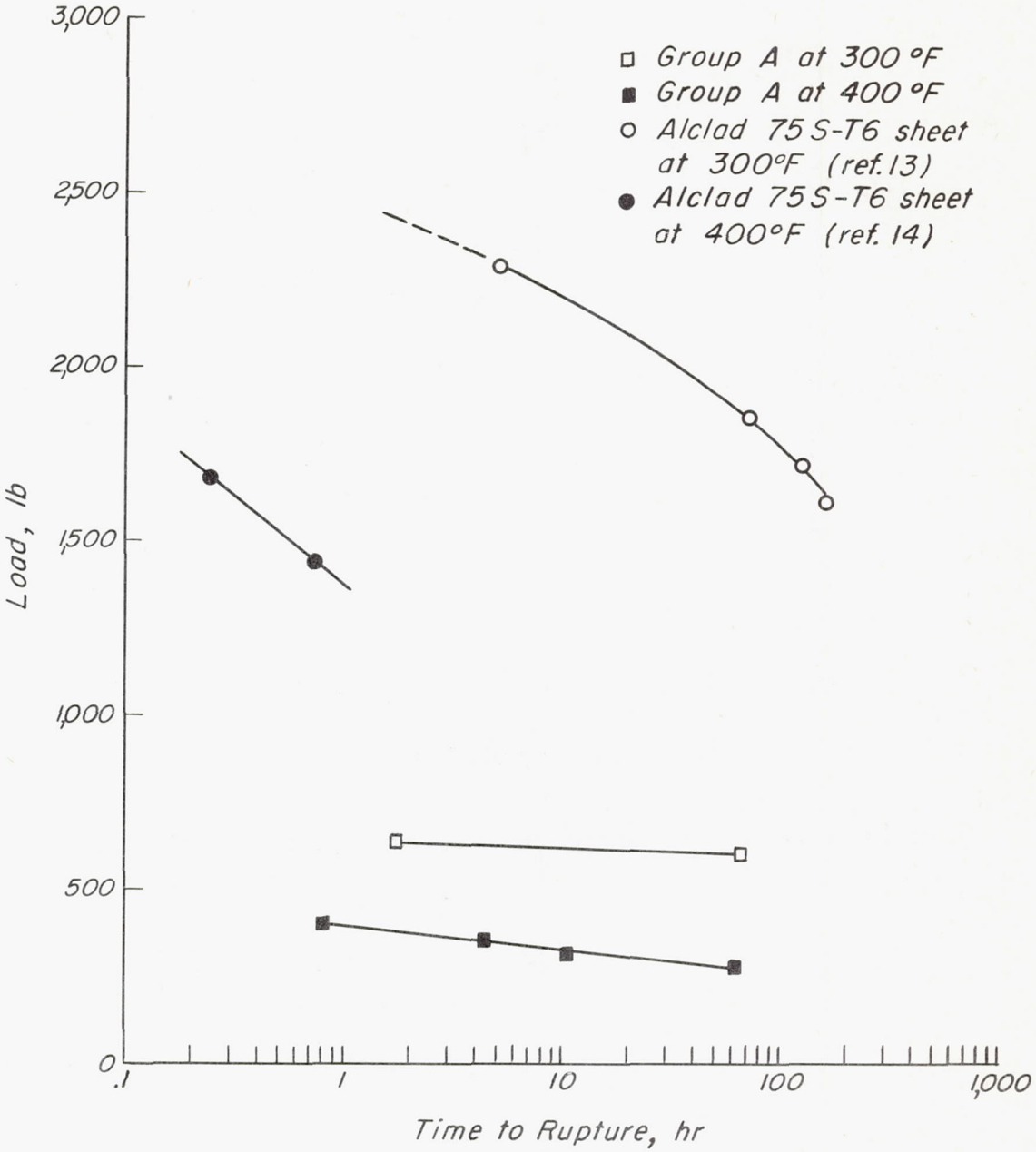

Figure 17.- Comparison of load-rupture curves of group A joints and alclad 75S-T6 sheet.

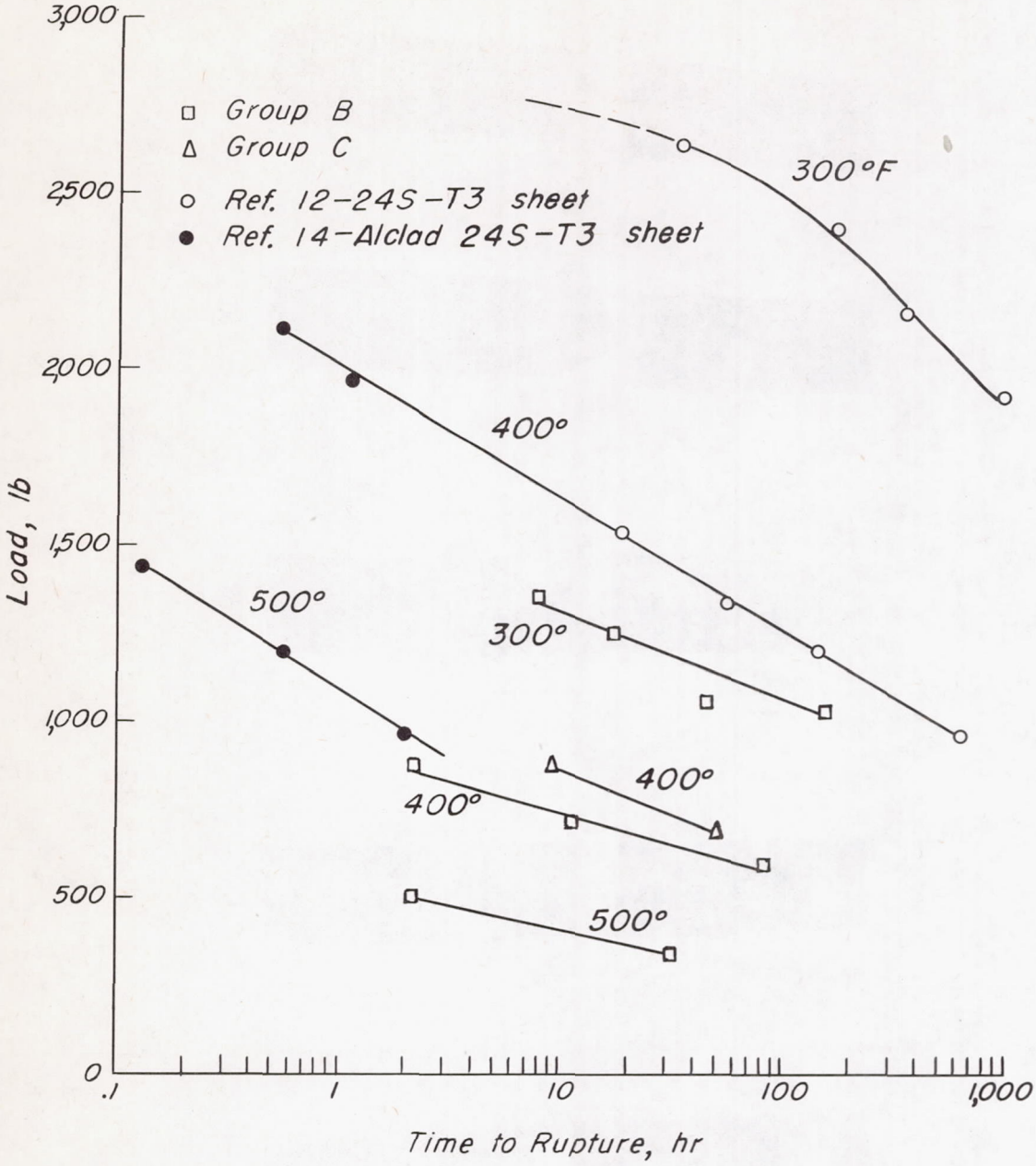

Figure 18.- Comparison of load-rupture curves of group B and group C joints and 24S-T3 sheet.

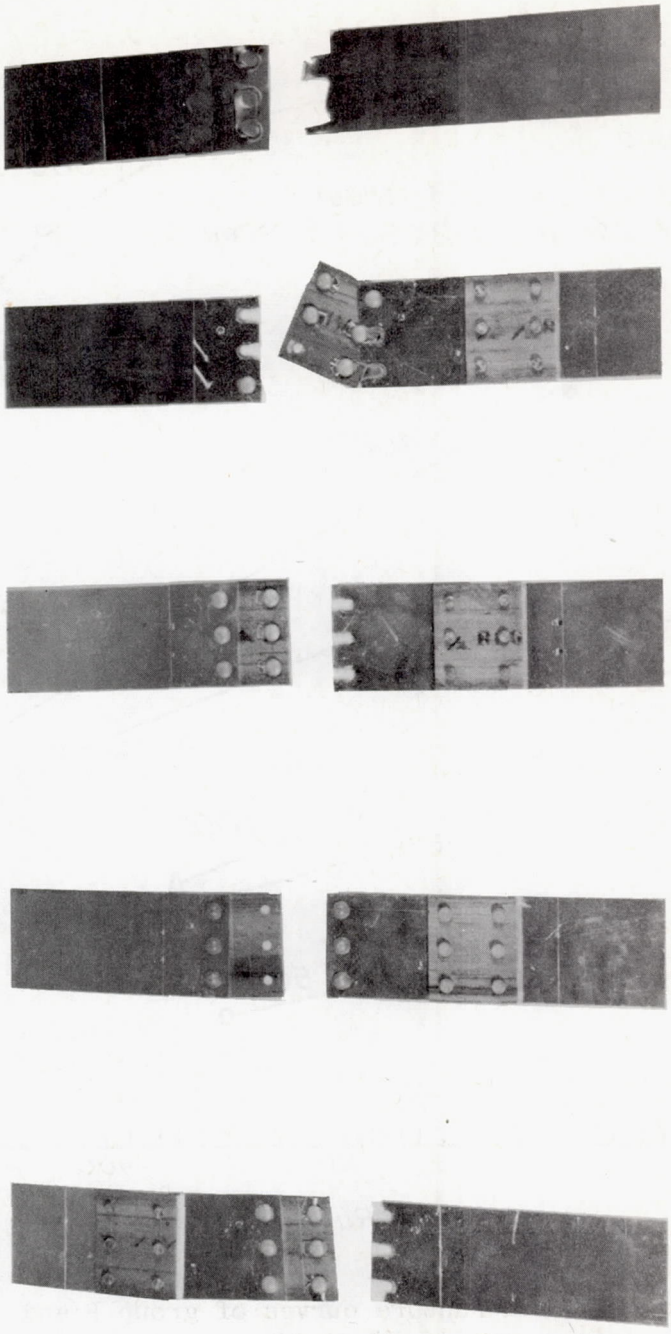

L-87901

Figure 19.- Typical joint failures.

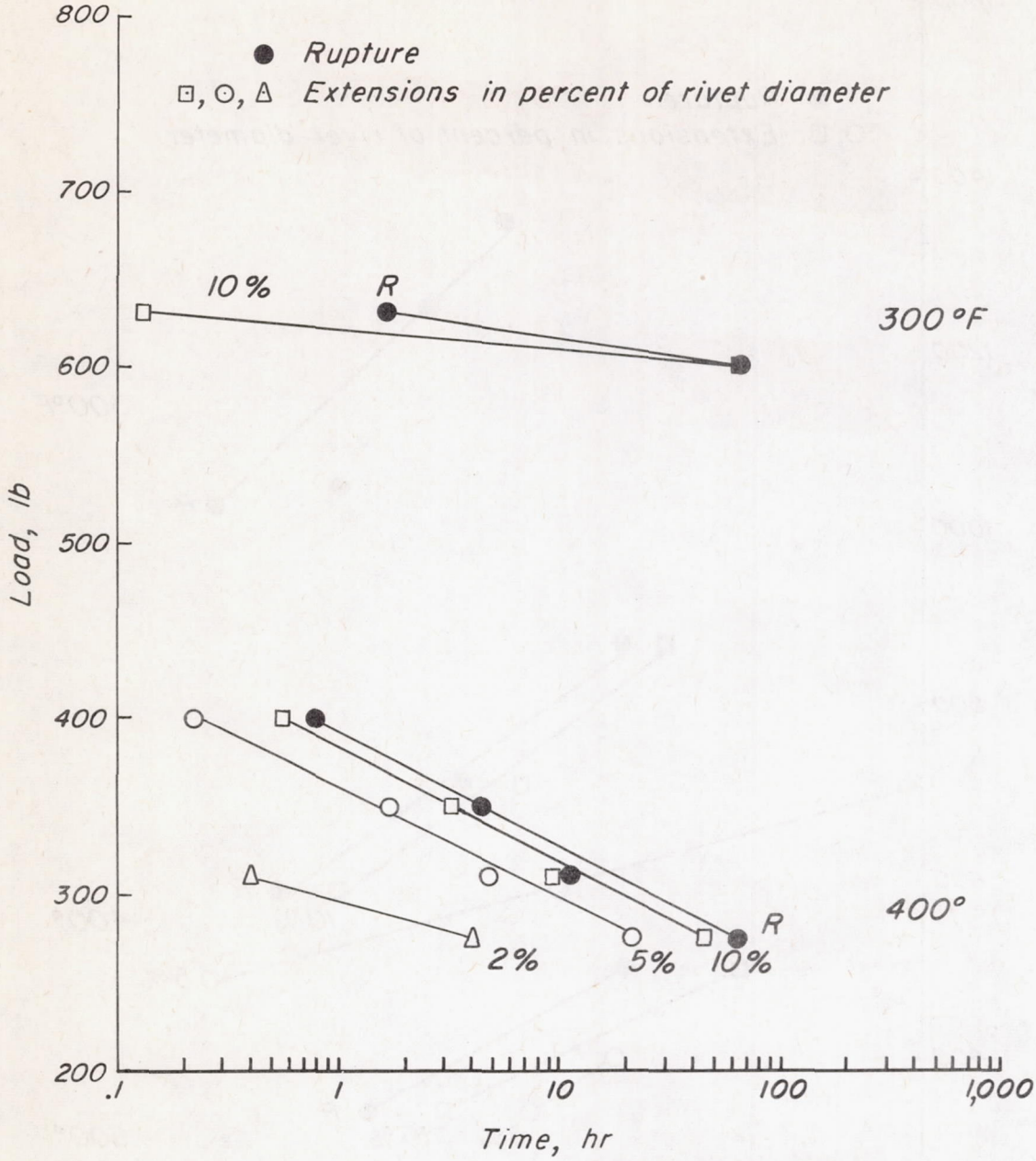

(a) Group A joints.

Figure 20.- Design curves.

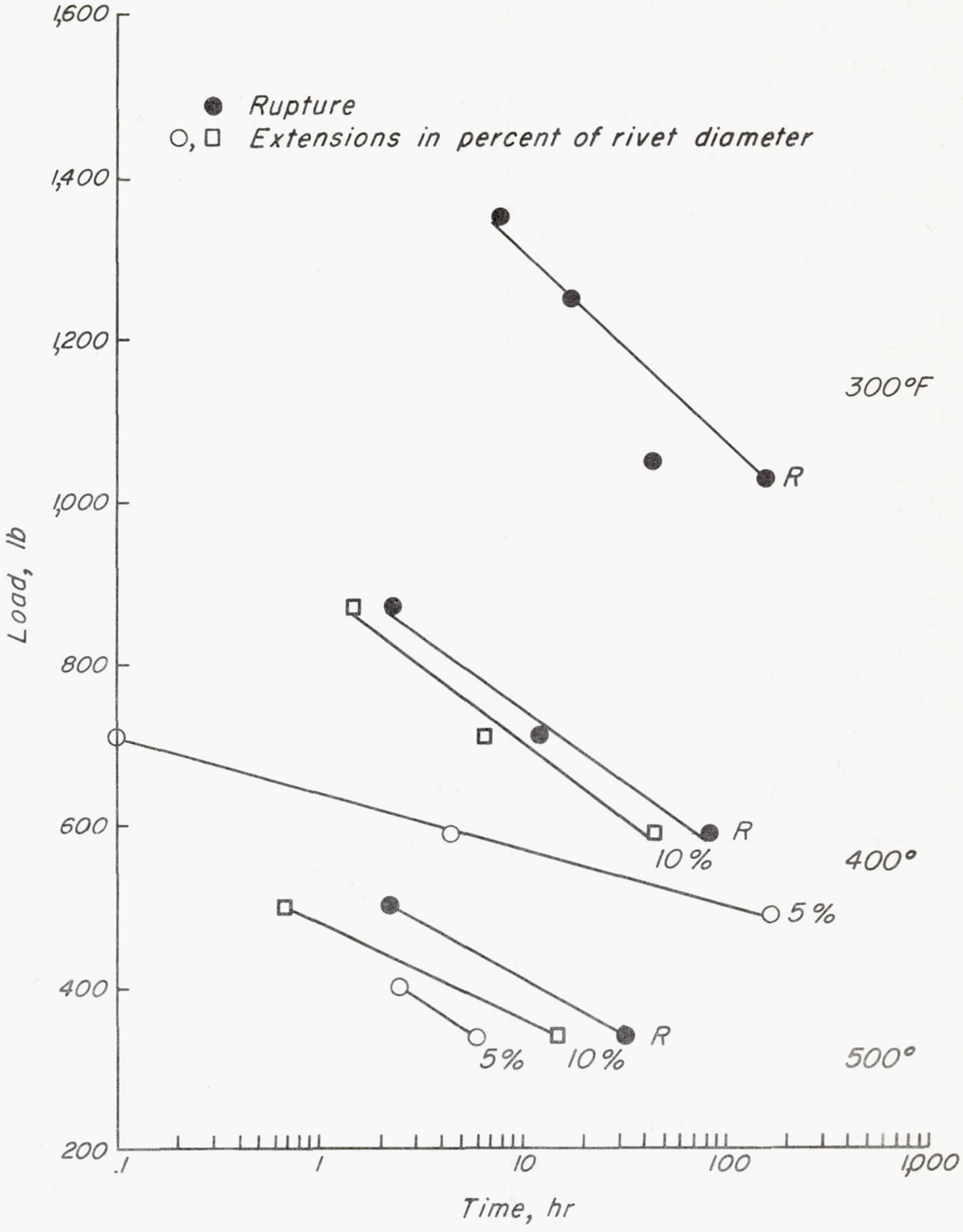

(b) Group B joints.

Figure 20.- Continued.

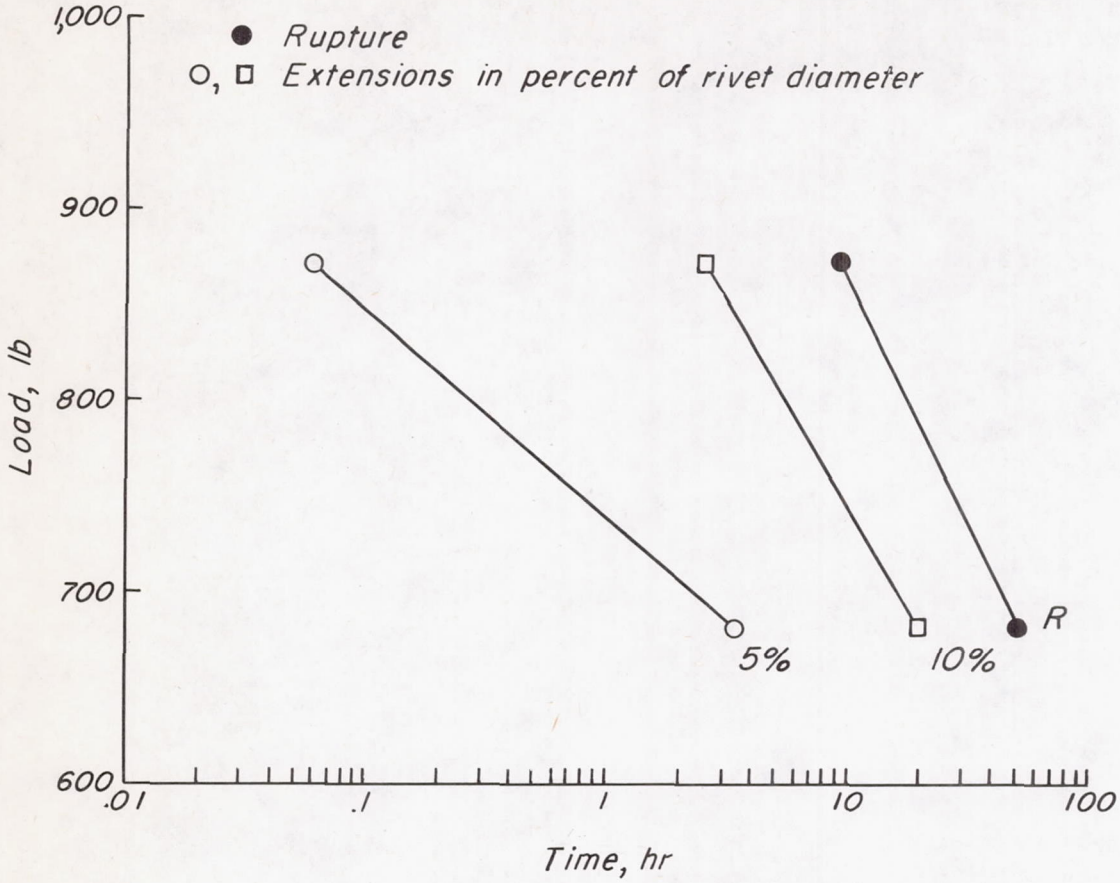

(c) Group C joints, 400° F.

Figure 20.- Concluded.